eLife

Biochemistry and Chemical Biology
Microbiology and Infectious Disease

Reviewed Preprint
v2 • June 14, 2024
Revised by authors

Reviewed Preprint
v1 • February 2, 2024

Chemoproteomics validates selective targeting of *Plasmodium* M1 alanyl aminopeptidase as an antimalarial strategy

Darren Creek, Carlo Giannangelo, Matthew Challis, Ghizal Siddiqui, Rebecca Edgar, Tess Malcolm, Chaille Webb, Nyssa Drinkwater, Natalie Vinh, Christopher MacRaild, Natalie Counihan, Sandra Duffy, Sergio Wittlin, Shane Devine, Vicky Avery, Tania de Koning-Ward, Peter Scammells, Sheena McGowan

Monash University • Deakin University • Griffith University • University of Basel • Walter and Eliza Hall Institute • Monash Institute of Pharmaceutical Sciences

Abstract

New antimalarial drug candidates that act via novel mechanisms are urgently needed to combat malaria drug resistance. Here, we describe the multi-omic chemical validation of *Plasmodium* M1 alanyl metalloaminopeptidase as an attractive drug target using the selective inhibitor, MIPS2673. MIPS2673 demonstrated potent inhibition of recombinant *Plasmodium* falciparum (*Pf*A-M1) and Plasmodium vivax (*Pv*A-M1) M1 metalloaminopeptidases, with selectivity over other *Plasmodium* and human aminopeptidases, and displayed excellent *in vitro* antimalarial activity with no significant host cytotoxicity. Orthogonal label-free chemoproteomic methods based on thermal stability and limited proteolysis of whole parasite lysates revealed that MIPS2673 solely targets *Pf*A-M1 in parasites, with limited proteolysis also enabling estimation of the binding site on *Pf*A-M1 to within ~5 Å of that determined by X-ray crystallography. Finally, functional investigation by untargeted metabolomics demonstrated that MIPS2673 inhibits the key role of *Pf*A-M1 in haemoglobin digestion. Combined, our unbiased multi-omic target deconvolution methods confirmed the on-target activity of MIPS2673, and validated selective inhibition of M1 alanyl metalloaminopeptidase as a promising antimalarial strategy.

eLife assessment

The manuscript makes an **important** contribution to antimalarial drug discovery, utilizing diverse systems biology methodologies. It focuses on an improved M1 metalloprotease inhibitor and provides **compelling** evidence for the utility of chemoproteomics in pinpointing PfA-M1 targeting. Additionally, metabolomic analysis reveals specific alterations in the final steps of hemoglobin breakdown. These findings highlight the potential of the developed methodology not only for PfA-M1 targeting but also for other inhibitors targeting various malarial proteins or pathways.

https://doi.org/10.7554/eLife.92990.2.sa3

Introduction

Malaria is a devastating parasitic disease that causes major health, economic and societal impacts to almost half of the world's population that live in malaria-endemic countries. In 2021 there were an estimated 247 million cases of malaria globally and 619 000 associated deaths.[1] An estimated 95% of malaria deaths are attributed to *P. falciparum*, the species responsible for the most severe and lethal form of the disease.[1] *P. vivax* is also responsible for significant morbidity, and is the most geographically widespread malaria parasite.[2] Although the global incidence rate of malaria has declined over the last decade, the number of people worldwide suffering and dying from malaria is now increasing and parasite resistance has emerged to all current antimalarial drug classes, including the front-line artemisinin therapies.[1,3] Alarmingly, artemisinin-based combination therapies fail to cure infections in up to 50% of patients in some regions of Asia[4] and delayed parasite clearance rates following artemisinin-based therapy (synonymous with decreased parasite susceptibility to artemisinin) has now been detected in Africa,[5] where most malaria deaths occur. This, combined with the lack of mechanistic diversity in emerging antimalarials in development, means there is an urgent need for new drug classes with novel mechanisms of action that bypass resistance and treat both *P. falciparum* and *P. vivax* infections.

Haemoglobin digestion is an essential metabolic process and a point of key vulnerability during *Plasmodium* parasite intraerythrocytic development. The parasite digests up to 75% of host cell haemoglobin to provide amino acids for protein synthesis and this process additionally serves non-anabolic functions, such as maintaining osmotic stability of the infected red blood cell.[6–9] *Plasmodium* parasites employ the interplay of numerous proteases from different classes to digest haemoglobin into its constituent amino acids.[10] *P. falciparum* M1 alanyl aminopeptidase (*Pf*A-M1) and M17 leucyl aminopeptidase (*Pf*A-M17) are two zinc-dependent metalloaminopeptidases involved in the terminal stage of haemoglobin digestion.[11,12] Both *Pf*A-M1 and *Pf*A-M17 are thought to be essential for parasite survival and are promising targets for antimalarial therapy *in vitro* and in vivo.[11–25] However, attempts at genetic manipulation of *Pf*A-M1 have been unsuccessful to date, which has precluded formal genetic validation of *Pf*A-M1 as a drug target. Bestatin-based inhibitors of *Pf*A-M1 were previously shown to prevent proteolysis of haemoglobin peptides, leading to a swollen digestive vacuole and stalled growth at the trophozoite stage.[15] Loss of *Pf*A-M17 function through chemical inhibition or conditional knockdown also results in stalled growth at the trophozoite stage but does not induce digestive vacuole swelling.[11] Instead, specific loss of *Pf*A-M17 function results in the presence of multiple membrane bound digestive vacuoles per parasite. We have previously used rational drug design to optimise dual M1 and M17 inhibitors with nanomolar potency across multiple *Plasmodium* species.[20,21,23,25] More recently, we reported a selective *Pf*A-M17 inhibitor with potent antimalarial activity.[11]

Like *Pf*A-M17, *Pf*A-M1 is an attractive target for novel antimalarial drug development. The *Pf*A-M1 enzyme is a monomeric protein consisting of four domains and is widely believed to function in the cytosol, although localisation to other compartments has been reported.[12,15,26-28] It has a broad substrate specificity that includes most basic and hydrophobic amino acids, but preferentially cleaves leucine and methionine.[26,29] *Pf*A-M1 uses a zinc-dependent mechanism to catalyse the release of single amino acids from the N-terminus of short peptides. All reported inhibitors of *Pf*A-M1 target the enzyme active site and act to chelate the catalytic zinc ion.[13,15,19-21,29-33] Obtaining selectivity for *Pf*A-M1 over *Pf*A-M17 is challenging as the enzymes share similar architecture within the active sites and a catalytic mechanism involving zinc ions.[30,34] As such, very few compounds that selectively inhibit *Pf*A-M1 over *Pf*A-M17 have been reported[15,18,31] and unbiased identification of the target in parasites is critical to confirm specificity.

Identifying the molecular targets of compounds is a significant challenge for antimalarial drug development.[35,36] One of the most successful approaches to target deconvolution has been *in vitro* evolution and whole genome analysis (IVIEWGA).[37–41] However, IVIEWGA can also point to genes encoding general drug-resistance mechanisms rather than the cellular target, and a major goal of new drug development for malaria is the identification of compounds that fail to yield resistant parasites *in vitro* (irresistible compounds), as these compounds are less likely to result in clinical resistance.[42] Chemoproteomics methods based on mass spectrometry offer alternative routes to validate the molecular target(s) of compounds in parasites. One strategy relies on the use of chemical probes to enrich and identify protein targets.[43] However, this method requires chemical modification of the drug, which could alter its pharmacological properties. New thermal stability[44,45] and limited proteolysis[46] techniques are two examples of unbiased chemoproteomics methods that provide direct evidence of on-target engagement on a proteome-wide scale, without the need for modification of the drug. These methods rely on the concepts of thermal and proteolytic stabilisation of the protein target due to ligand binding and leverage recent advances in mass spectrometry to detect drug-specific changes to protein or peptide abundance within complex proteomes. Thermal proteome profiling was recently applied in *P. falciparum* to successfully identify the targets of several antimalarial compounds.[45,47] Whereas limited proteolysis proteomics has not previously been reported to identify drug targets in *P. falciparum*, this approach has successfully mapped protein-small molecule interactions in other complex eukaryotic proteomes.[46]

Here, we report an M1 selective aminopeptidase inhibitor with a hydroxamic acid zinc binding group[20] (MIPS2673), which targets both the *P. falciparum* (*Pf*A-M1) and *P. vivax* (*Pv*A-M1) M1 homologues and demonstrates antimalarial activity against a panel of drug resistant *P. falciparum* strains. We developed orthogonal chemoproteomics approaches based on thermal stability and limited proteolysis, combined with metabolomics analysis, to validate the on-target activity of MIPS2673 in parasites. Our comparatively simple and inexpensive chemoproteomics methods for identifying antimalarial drug targets utilise an efficient data-independent acquisition mass spectrometry (DIA-MS) approach that allows comprehensive and reproducible proteome coverage. Together, our studies confirm *Plasmodium* M1 alanyl aminopeptidase as the target of MIPS2673 and validate selective inhibition of this enzyme as a potential multi-stage and cross-species antimalarial strategy.

Results

Design and synthesis of a cross-species hydroxamic acid-based inhibitor selective for *Plasmodium* M1 alanyl aminopeptidase

We previously reported a series of *Pf*A-M1 and M17 aminopeptidase inhibitors that possessed a hydroxamic acid zinc binding group to coordinate catalytic zinc ion(s) and a variety of hydrophobic groups to probe the S1' binding pocket of these enzymes.[21] Whilst a number of these modifications successfully improved inhibitory potency, their incorporation reduced polarity and aqueous solubility. One such example is the pivaloyl group present in compound **1** (**Fig. 1A**).[20,21] In order to balance these opposing factors, one of the methyl groups of the pivaloyl was replaced by an alcohol to increase polarity whilst maintaining the capacity to engage the S1'-pocket via hydrophobic interactions (**Fig. 1A**). This modification resulted in MIPS2673 (compound **4**), which has a significantly lower cLogP (1.45 vs 2.23 for **1**) and favourable solubility (i.e. the kinetic solubility of MIPS2673 was estimated to be in the 50-100 mg/mL range using nephelometry vs 12.5-25 µg/mL for 1). MIPS2673 (**4**) was synthesized from methyl 2-amino-2-(4-bromophenyl)acetate (**2**) in three synthetic steps as shown in **Figure 1**. Amide formation was achieved via an EDCI-mediated coupling and the trifluorophenyl moiety was installed using a Suzuki-Miyaura coupling to form the synthetic intermediate **3**. Finally, the methyl ester was converted to the corresponding hydroxamic acid using 5 M methanolic KOH and NH_2OH•HCl to afford MIPS2673 (**4**).

We determined the inhibitory activity of MIPS2673 against M1 and M17 enzymes from both *P. falciparum* and *P. vivax* (**Fig. 1B**). The binding affinities (*K*i) of MIPS2673 toward purified, recombinant *Pf*A-M1 shows the compound to be a potent inhibitor (*K*i = 211 ± 11 nM), with >4-fold selectivity over *Pf*A-M17 (*K*i = 921 ± 69 nM). MIPS2673 was significantly more potent against *Pv*A-M1 (*K*i = 6.4 ± 0.5 nM) with >155-fold selectivity over *Pv*A-M17 (*K*i >1000 nM). We confirmed that MIPS2673 is non-inhibitory against the *Pf*A-M18 (*K*i >500 µM) and *Pf*APP (*K*i >40 µM) recombinant metalloaminopeptidases (data not shown).

In contrast to the M1 selectivity demonstrated by MIPS2673, the inhibitor **1** was 2-fold more selective for *Pf*A-M17 vs *Pf*A-M1.[21] When bound to *Pf*A-M1, the position of the biaryl of MIPS2673 compares with that of our previous inhibitors.[20,21] The moiety makes similar interactions with Met1034 (hydrophobic) and Glu319 (carbonyl-pi) (**Fig. 1B**). The fluoro-substituents sit deep in the S1 pocket and form the same intricate network of water-mediated hydrogen-bonds as **1**, in which the fluorine atoms act as H-bond acceptors. The substitution on the *tert*-butyl, replacing a methyl with an alcohol, is difficult to definitively position in the structure due to the rotation around the C-03 bond. It is possible that this alcohol could form a long H-bond to Arg-489, which should provide some improvement in position and potency. The Arg-489 side-chain shows two orientations in the electron density, suggesting that some rotation of the alcohol is occurring (**Fig. 1B**). Inspection of the structure of *Pf*A-M17 with **1** (PDB ID 4ZY2)[20] does not reveal why the compound is selective. The *tert*-butyl of **1** is sitting in an open pocket and the introduction of an alcohol is unlikely to induce any clashes, steric or electrostatic. This suggests that the reason for the selectivity between the two enzymes results from the ability (or inability) to access the interior cavity of the *Pf*A-M17 hexamer that houses the active sites.

To investigate the potential for off-target effects, we examined the selectivity of MIPS2673 over several human M1 homologs, including leukotriene A-4 hydrolase (LTA4H), endoplasmic reticulum aminopeptidase 1 (ERAP1) and endoplasmic reticulum aminopeptidase 2 (ERAP2). MIPS2673 showed minimal inhibition of ERAP1 and ERAP2 at concentrations below 500 µM (Table S1), whereas MIPS2673 caused >50% inhibition of LTA4H at concentrations above 10 µM (Table S1). We also tested MIPS2673 against the HEK293 cell line to further predict potential human cytotoxicity. No cytotoxicity to HEK293 cells was observed up to a concentration of 40 µM. As a comparison, the current antimalarials chloroquine and dihydroartemisinin inhibit HEK293 proliferation by 67% and 29%, respectively, at 40 µM. At 120 µM, MIPS2673 inhibited cellular proliferation by 89% compared to the untreated control (Table S2).

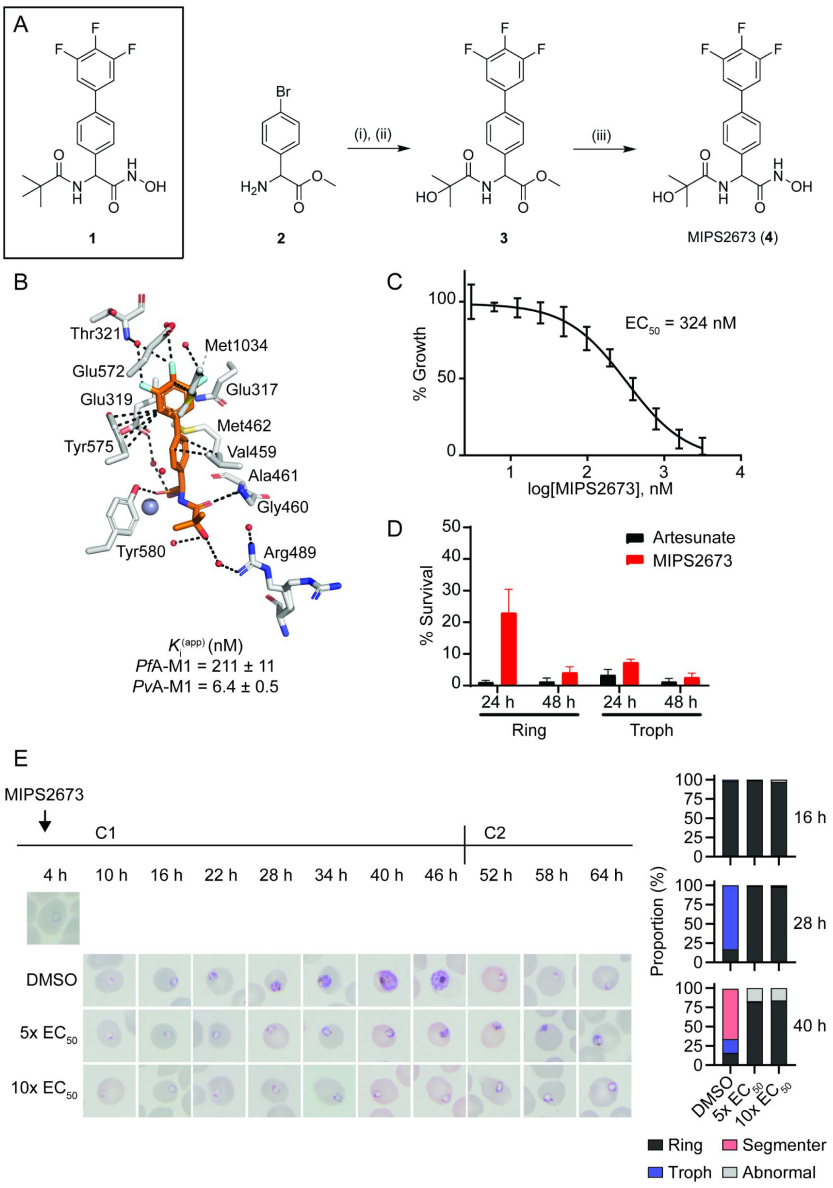

Figure 1

Synthesis and antimalarial activity of the M1-selective aminopeptidase inhibitor, MIPS2673.

(A) Synthesis of MIPS2673 (**4**). *Reagents and conditions*: (i) RCOOH, EDCI, DMAP, CH_2Cl_2; (ii) 3,4,5-trifluorophenylboronic acid, $Pd(PPh_3)_2Cl_2$, Na_2CO_3, THF; (iii) NH_2OH•HCl, KOH. (B) Binding mode of MIPS2673 bound to *Pf*A-M1 determined by X-ray crystallography (8SLO.pdb). Interactions between MIPS2673 (orange sticks) and *Pf*A-M1 (grey) shown as black dashed lines. Inhibition constant (*Ki*) for MIPS2673 toward recombinant, purified *Pf*A-M1 and *Pv*A-M1. (C) Sensitivity to MIPS2673 exposure (72 h) for P. falciparum 3D7 parasites. Parasite growth was determined relative to a no-drug control by SYBR Green I assay. The EC_{50} value was calculated from 4 biological replicates performed in technical triplicate and the data plotted as the mean ± standard error of the mean. (D) Stage-dependent activity of MIPS2673 in *P. falciparum* (3D7). Synchronised ring- or trophozoite-stage cultures were incubated for either 24 or 48 h with compound at 10x EC_{50}, before the drug was washed off and parasites allowed to grow for a further 48 hours. Growth was determined via Sybr Green I assay and compared to vehicle (DMSO)-treated controls. Shown is the mean ± standard deviation (n=4). (E) MIPS2673-induced morphology and growth effects for *P. falciparum* 3D7 parasites (left). Synchronised cultures at 4 h post-invasion were treated over two cycles (C1, cycle 1; C2, cycle 2) with either 5x or 10x EC_{50} or DMSO at the concentration present in the 10x EC_{50} treatment. Representative Giemsa-stained smears from 2 biological replicates show parasites stalling and dying at the ring to trophozoite transition. The percentage of parasites at each stage of development is shown from counts of 100 infected red blood cells at 16 h, 28 h and 40 h post invasion (right).

In vitro antiparasitic activity of MIPS2673

Having synthesised a *Plasmodium* specific M1 aminopeptidase inhibitor, we next explored the activity of MIPS2673 against *in vitro* blood-stage cultures of *P. falciparum*. We found that MIPS2673 has a 72 h EC_{50} of 324 nM (250-470 CI) against the laboratory reference strain, 3D7 (**Fig. 1C**), compared with the expected low nanomolar EC_{50} achieved with the clinically used artemisinin derivative, artesunate, which was analysed in parallel (**Fig. S1**). MIPS2673 demonstrated no shift in EC_{50} when tested against a panel of drug resistant *P. falciparum* lines (**Table S3**). Stage specificity assays were performed to identify which stage of asexual development MIPS2673 is most active against. Synchronised ring or trophozoite cultures were exposed to MIPS2673 for 24 h or 48 h at 10x EC_{50}, then stringently washed to remove the compound. Parasite growth was assessed after 48 h compared to a vehicle-treated control. This confirmed MIPS2673 is most potent against trophozoite stage parasites (**Fig. 1D**), corresponding to the period of peak *Pf*A-M1 expression[26] and activity.[48] As expected, no stage-dependent difference in activity was observed in parasites exposed to MIPS2673 for 48 h, as this duration incorporates the full asexual erythrocytic cycle. The control compound, artesunate, was equipotent across all conditions, consistent with the known activity and kinetic profiles for artemisinins.[49]

To visually characterise the effects of MIPS2673 on parasites, we treated synchronised 3D7 cultures at the early ring stage and monitored their development by light microscopy evaluation of Giemsa-stained thin blood smears (**Fig. 1E**). We found that MIPS2673 caused significant growth retardation when compared to the untreated control and parasite growth stalled at the ring to trophozoite transition (~16-22 h post invasion). In contrast, untreated parasites progressed into schizonts and eventually re-invaded red blood cells to commence the next asexual cycle.

Having confirmed activity against asexual stages of *P. falciparum*, we next determined whether MIPS2673 kills the transmissible sexual forms of the parasite, known as gametocytes. We found that MIPS2673 has transmission-blocking activity and is most potent against early gametocytes (stages I-III), compared to late (stages IV-V) and mature (stage V) stages (**Table S4**), but is less potent than the artemisinin derivative, artesunate.

Identification of molecular targets for MIPS2673 in *P. falciparum* by thermal stability proteomics

Our biochemical studies showing binding and inhibition of recombinant *Plasmodium* metalloaminopeptidases do not rule out the possibility that the anti-parasitic activity of MIPS2673 is due to non-specific binding to other parasite metalloproteins or off-target proteins. Genetic target validation was not possible as previous attempts to mutate *Pf*A-M1 were not successful,[12,50] and MIPS2673-resistant parasites were not available. Therefore, we developed orthogonal mass spectrometry-based chemoproteomics approaches to validate that MIPS2673 is on-target and M1-selective in the complex parasite environment (**Fig. 2**). We initially developed a streamlined thermal stability proteomics workflow that combined traditional thermal proteome profiling methods with an optimised data-independent acquisition (DIA)-LC-MS/MS approach.[51,52]

To identify the binding target/s of MIPS2673 in *P. falciparum* asexual blood stages in a proteome-wide manner, we used native parasite lysates, as direct drug-protein interactions are more selectively identified in cellular lysates, rather than live cells that are susceptible to downstream effects of drug action. The parasite lysates were exposed to 1 μM or 4 μM of MIPS2673 or vehicle (DMSO control) for 3 minutes prior to heating at 60 °C, a temperature that should allow detection of most drug-induced protein stabilisation events in an untargeted manner with wide proteome coverage.[45,53] After the thermal challenge, the soluble (non-denatured) protein fraction was isolated by ultracentrifugation, digested overnight with trypsin and the peptide mixture analysed directly using global DIA-LC-MS/MS. Proteins detected with significantly higher abundance in

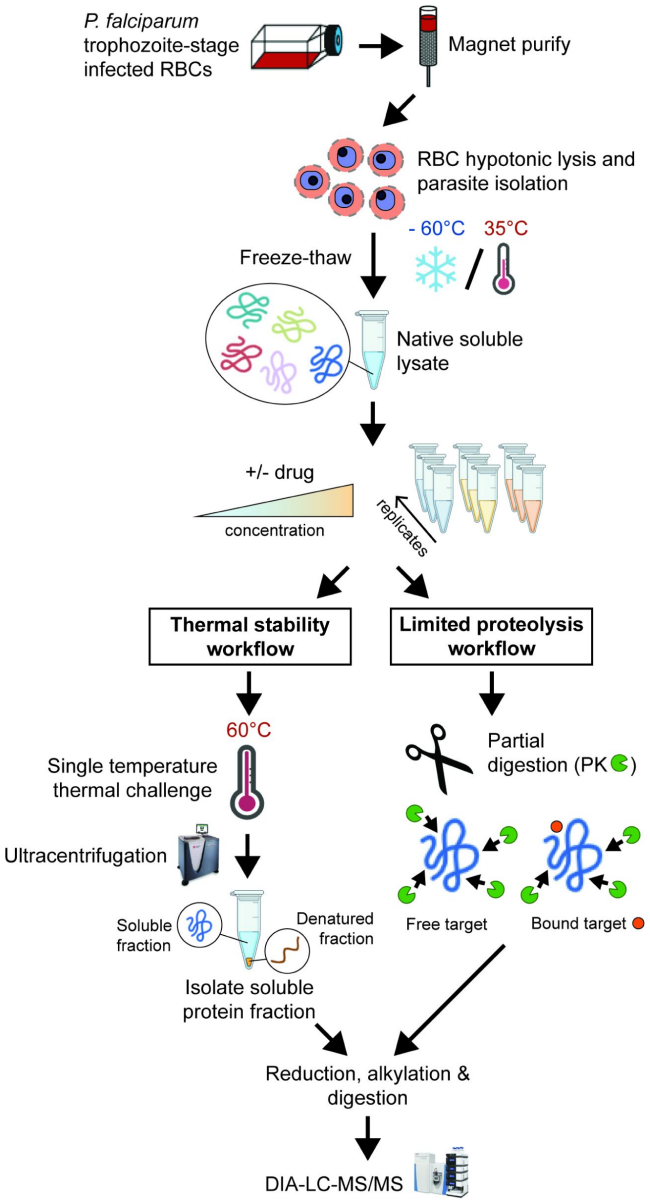

Figure 2

Experimental thermal stability and limited proteolysis workflows for unbiased drug target identification in *P. falciparum* lysates.

Synchronised trophozoite-stage parasites (30-38 h post invasion) are isolated from the host red blood cell by hypotonic lysis. Proteins are extracted from cells under native conditions by multiple freeze-thaw cycles. The lysate, comprising the soluble protein fraction, is pooled and distributed to achieve multiple independent incubations per reaction condition for use in either thermal stability or limited proteolysis workflows. For thermal stability proteomics studies, the parasite lysate is subjected to treatment with vehicle (untreated control) or drug at two concentrations, followed by thermal challenge at 60 °C. The soluble (non-denatured) protein fraction is isolated by ultracentrifugation and digested overnight with trypsin. The resulting peptide mixture is analysed by DIA-LC-MS/MS against an in-house generated spectral library to determine drug-induced thermal stabilisation. For limited proteolysis studies, ligand-protein interactions are monitored at multiple drug concentrations following double protease digestion. An initial pulse proteolysis with the broad specificity protease, proteinase K (PK), captures local ligand-induced structural alterations of proteins that become differentially susceptible to protease cleavage upon drug binding. Samples then undergo complete digestion under reducing conditions with trypsin/LysC. Differential proteolytic patterns produced upon ligand binding are detected by DIA-LC-MS/MS and analysed against a limited proteolysis spectral library.

treated relative to control samples reflect thermal stabilisation of the target due to ligand binding. To minimise identification of false positive hits, proteins reproducibly stabilised ($p<0.05$ and fold-change ≥1.2 compared to the untreated control) across multiple drug concentrations and experiments were considered drug interacting proteins. Among 1632 proteins reproducibly detected with a minimum of two peptides across two independent experiments (each with at least three independent incubations of MIPS2673 or vehicle with protein lysate), five proteins were consistently stabilised at both drug concentrations compared to DMSO (**Fig. 3A**, **Data S1** and **Data S2**). Of these, *Pf*A-M1 (PF3D7_1311800) was one of the most significantly stabilised proteins ($p<0.01$ at 1 μM). *Pf*A-M1 exhibited concentration-dependent stabilisation in the presence of MIPS2673, with an average stabilisation of 1.8-fold and 2.8-fold at 1 μM and 4 μM, respectively, relative to the untreated control (**Fig. 3B**). The four other proteins consistently stabilised were not metalloproteins and included two conserved *Plasmodium* proteins with unknown functions (PF3D7_1026000 and PF3D7_0604300), a putative AP2 domain transcription factor (PF3D7_1239200) and a human protein, Ras-related Rab-39A (Q14964) (**Fig. 3B**). These hits could represent other MIPS2673-interacting proteins. The *Pf*A-M17 protein was not stabilised by MIPS2673 at either drug concentration after a 60 °C thermal challenge (**Fig. S2**). We previously showed *Pf*A-M17 is stabilised at this temperature in parasite lysates treated with a selective *Pf*A-M17 inhibitor.[11] Overall, our unbiased thermal stabilisation proteomics approach confirmed MIPS2673 selectively targets the M1 aminopeptidase over M17 and does not bind indiscriminately to parasite metalloproteins.

Identification of MIPS2673 targets in *P. falciparum* by limited proteolysis coupled mass spectrometry

Having identified several MIPS2673 binding proteins using thermal stability proteomics, we wanted to further investigate the target profile of MIPS2673 with a complementary target deconvolution method. To this end, we developed an efficient protocol for limited proteolysis-based studies of *P. falciparum* and applied it for the unbiased identification of targets of MIPS2673 (**Fig. 2**). Native *P. falciparum* lysates were treated for 10 minutes with different concentrations of MIPS2673 (1 μM or 10 μM in experiment one and 0.1 μM, 1 μM or 10 μM in experiment two) or vehicle in at least four independent incubations per experiment. Proteome extracts were then subjected to double protease digestion. An initial limited proteolysis with proteinase K for 4 minutes captured local structural alterations of proteins that become differentially susceptible to protease cleavage upon drug binding. Secondly, samples undergo complete digestion under reducing conditions overnight with trypsin/LysC to make peptides amenable for global proteomics analysis. Differentially abundant proteolytic peptides between MIPS2673 and vehicle-treated samples were then identified on a global scale with DIA-LC-MS/MS. The proteolytic peptide patterns of drug targets should be altered in the treated samples as compound binding prevents protein cleavage by proteinase K, resulting in decreased abundance of peptides with non-tryptic ends or an increase in concentration of the associated fully tryptic peptide (**Fig. 4A**). We quantified 26,611 peptides from 2,153 proteins in experiment one and 16,662 peptides from 1,989 proteins in experiment two (**Data S3**). Each dataset was initially analysed for differentially abundant peptides between each MIPS2673 concentration and vehicle by filtering based upon relative peptide abundance (absolute fold-change >1.5), statistical significance ($q<0.01$) and proteolytic peptide pattern (i.e. increased fully tryptic or decreased half tryptic). In experiment one and experiment two respectively, approximately 3% of peptides from 379 proteins and 0.6% of peptides from 69 proteins, met these thresholds at each drug concentration and were considered significant (**Fig. 4B**). After prioritising targets based upon the number of significant peptides detected per protein (Fisher exact test, Bonferroni corrected $p<0.05$), we identified seven putative drug targets in experiment one and only one putative target in experiment two (**Fig. 4C** and **Data S4**). Interestingly, among the seven possible target proteins identified by limited proteolysis in experiment one, five were metalloproteins. These included *Pf*A-M1, three other aminopeptidases - M17 leucyl aminopeptidase, aminopeptidase P (*Pf*APP) and M18 aspartyl

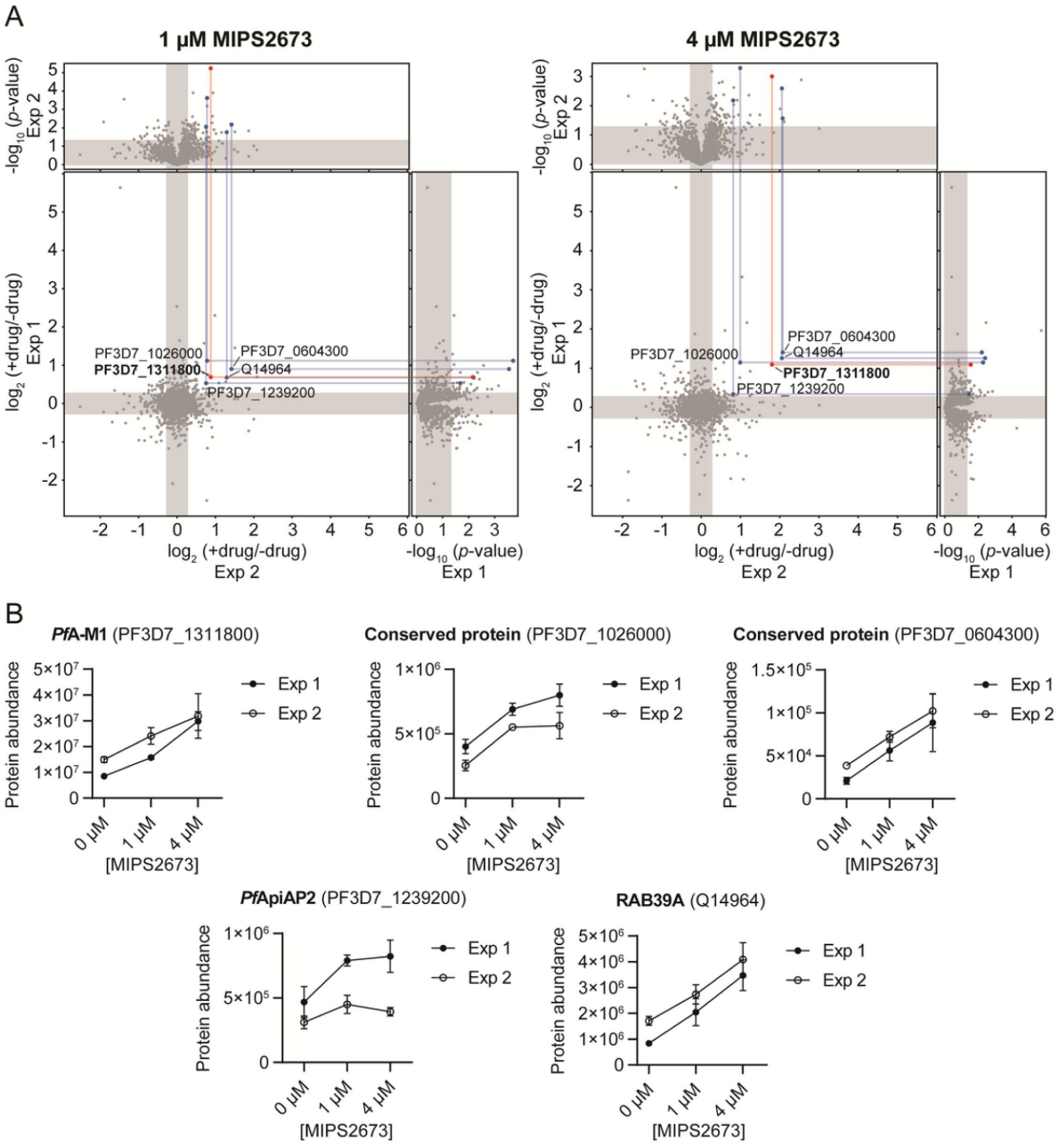

Figure 3

Thermal stabilisation of proteins by MIPS2673.

(A) Paired volcano plots of all proteins detected after a 60 °C thermal challenge across two experiments from *P. falciparum* lysates (at least n=3 of independent lysate incubations per condition and experiment) treated with 1 µM (left) and 4 µM (right) MIPS2673. Outside panels show the fold-change in protein abundance for treated relative to untreated samples as a function of statistical significance (p-value) for independent experiments. Each protein is represented with a single data point. Significance cut-offs for thermal stabilisation were p<0.05 (Welch's t test) and fold-change >1.2 (unshaded regions). The central panel plots protein fold-change from experiment one and two, with proteins in the upper right quadrant reproducibly stabilised by >1.2-fold. Proteins passing both fold-change and statistical cut-offs at both drug concentrations and in multiple independent experiments are highlighted. M1-family alanyl aminopeptidase (PF3D7_1311800) is in red and all other proteins passing cut-offs are in blue. (B) Individual profiles for the five proteins reproducibly stabilised by MIPS2673 after a 60 °C thermal challenge. Two independent experiments are shown. Data are mean protein abundances in the absence and presence of MIPS2673 (± SD) from 4 replicates.

aminopeptidase (*Pf*A-M18) - and adenosine deaminase (*Pf*ADA) (**Fig. 4C**). The expected target, *Pf*A-M1 aminopeptidase, was the only protein reproducibly identified as the MIPS2673 target across both independent limited proteolysis experiments. Indeed, the consistent identification of *Pf*A-M1 as the only significant protein in both LiP-MS and thermal stability proteomics methods strongly supports *Pf*A-M1 being the primary target of MIPS2673.

Features of structurally significant *Pf*A-M1 LiP-MS peptides

The identification of drug targets with LiP-MS typically identifies structurally perturbed peptides located in very close proximity to the ligand binding site[46,54] and we hypothesised that this would also be the case in our study. Among the 108 *Pf*A-M1 peptides reproducibly detected across both LiP-MS experiments we identified nine structurally significant LiP-MS peptides (q<0.01 and absolute fold-change >1.5 at all drug concentrations in both experiments) (**Fig. 5A**) and mapped these to our *Pf*A-M1 crystal structure with MIPS2673 bound (PDB ID: 8SLO). We measured the minimum distance between atoms of the significant peptides and those of MIPS2673 and found that structurally significant peptides identified with LiP-MS were frequently located in very close proximity to MIPS2673. The median minimum distance between the significant LiP-MS peptides and bound MIPS2673 was 6.5 Å, significantly less than the 13.2 Å median distance for all detected *Pf*A-M1 peptides (p=0.025) (**Fig. S3**). Among the nine structurally significant LiP-MS peptides, four contained atoms within Van der Waals distance (<4 Å) of MIPS2673. In contrast, the median minimum distance of structurally perturbed LiP peptides of other putative MIPS2673-interacting proteins identified with either thermal stability proteomics or LiP-MS (experiment 1) were not significantly closer to expected binding sites when compared to all peptides detected, except for significant LiP peptides from *Pf*A-M17 (median minimum distance of 8.56 Å vs 17.47 Å, p=0.045) (**Fig. S4**). Based on these observations, we hypothesised that significantly dysregulated LiP-MS peptides could estimate the known MIPS2673 binding site on *Pf*A-M1. A distance of 6.44 Å from MIPS2673 was used to define the binding cleft boundary[54] and included the *Pf*A-M1 residues known to interact with bound MIPS2673. Six of the nine significant LiP peptides overlapped with, or were within 4 Å of this binding cleft. The median distance between the atoms of significant LiP peptides and of cleft residues was 2.6 Å, compared to a median distance of 8.2 Å for all *Pf*A-M1 peptides (p=0.029) (**Fig. 5B**). Of the three significant LiP peptides located >4 Å from the operational binding site, two are located at the C-terminal opening in domain IV that forms a channel leading towards the active site.[30] To understand if this type of data could approximate a ligand binding site correctly, we calculated the centre of mass of the atoms of the nine structurally significant LiP peptides and represented this as a geometric point within the *Pf*A-M1 structure and then compared this to the known binding site (**Fig. 5C**). The minimum distance between this point and MIPS2673 was 5.2 Å and the MIPS2673 centre of mass neighbourhood (residues within 6.44 Å of the centre of mass) overlapped with the binding site (**Fig. 5C**). This indicated that our LiP-MS approach provides a good approximation of the MIPS2673 binding site with its target, *Pf*A-M1.

Untargeted metabolomics analysis of *P. falciparum* infected red blood cells treated with MIPS2673

To further determine the specificity of MIPS2673 for *Pf*A-M1 and whether it induces off-target effects, we performed untargeted metabolomics on infected red blood cells treated with 1 µM of MIPS2673 (3x EC_{50} value) for 1 h and compared the profile to vehicle (DMSO) control (4-9 biological replicates). Heatmap analysis of relative abundances of all putative metabolites revealed that treatment with MIPS2673 disproportionally impacted peptide metabolism (**Fig. S5**). Of the 201 putative peptides identified, 97 were significantly dysregulated (p<0.05). The majority of dysregulated peptides were significantly increased (fold-change >1.5 and p<0.05) in abundance in MIPS2673 treated cultures compared to DMSO control, indicative of aminopeptidase inhibition. Targeted analysis of the 97 increased peptides in drug treated cultures revealed that the

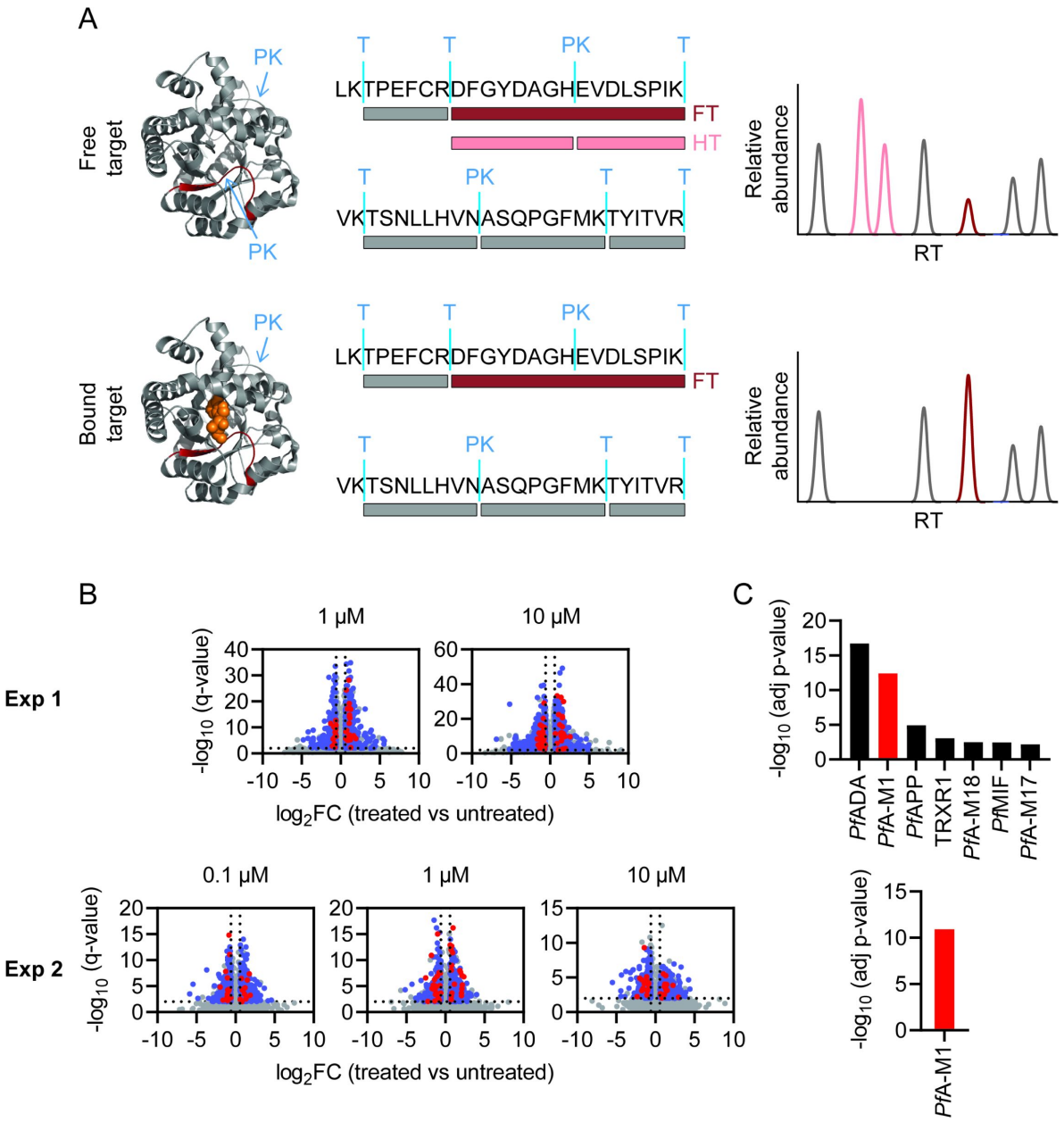

Figure 4

Identification of MIPS2673 target proteins using LiP-MS.

(A) Principle of LiP-MS analysis. Ligand binding to a protein alters the local proteolytic susceptibility and prevents protein cleavage by proteinase K. In the bound state this results in decreased abundance of peptides with non-tryptic ends (half tryptic, HT) shown in pink and/or an increase in concentration of the corresponding fully tryptic (FT) peptide, shown in red. Peptides unaffected by ligand binding (grey) are unchanged in abundance. (B) Volcano plots of two independent LiP-MS experiments (at least n = 3 independent lysate incubations per condition and experiment). Each data point represents a detected peptide. Fold-changes (FC) in peptide abundance in treated vs untreated samples are shown as a function of significance (q<0.01) at the MIPS2673 concentrations shown. Peptides highlighted in blue represent LiP peptides that were significant across all concentrations tested within an experiment. Red peptides represent significant LiP peptides from *Pf*A-M1. (C) Short-list of putative MIPS2673 targets identified in each LiP-MS experiment after prioritising targets based upon the number of significant peptides detected per protein. Significance was determined using a Fisher exact test and Bonferroni corrected p<0.05. The expected target *Pf*A-M1 aminopeptidase is shown in red.

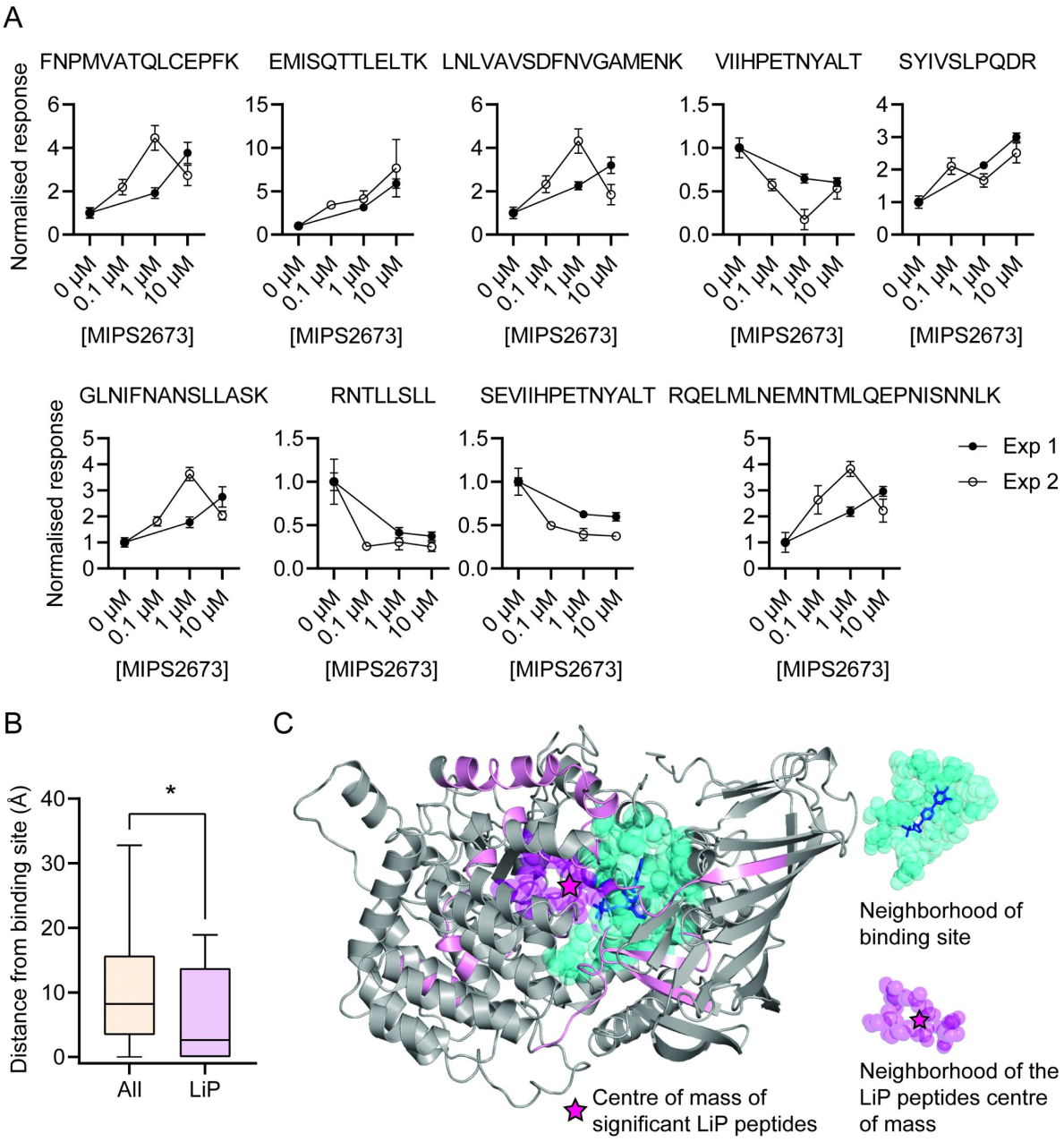

Figure 5

Features of structurally significant *Pf*A-M1 LiP-MS peptides.

(A) Relative abundance of the significant LiP peptides commonly identified across two LiP-MS experiments following *P. falciparum* proteome lysate treatment with MIPS2673. The mean ± SEM of at least three independent lysate incubations per condition and experiment are shown. (B) Median distances between atoms of the nine significant LiP peptides or all detected *Pf*A-M1 peptides and the *Pf*A-M1 binding cleft residues. *p<0.05, Mann-Whitney test. (C) MIPS2673 binding site on *Pf*A-M1 determined by X-ray crystallography (PDB: 8SLO), and approximation of the MIPS2673 binding site using the significant *Pf*A-M1 LiP peptides and centre of mass calculation. The significant LiP peptides are mapped onto the *Pf*A-M1 structure with MIPS2673 bound and are shown in pink. The drug ligand is shown in blue and the centre of mass of the significant LiP peptides is shown by a magenta star. The area in cyan represents the neighbourhood of the drug binding site determined as residues within 6.44 Å of bound MIPS2673. The neighbourhood of the LiP peptide centre of mass (residues within 6.44 Å of the centre of mass) is depicted in magenta.

majority were likely derived from haemoglobin (Hb) chains (α and β) (**Fig. 6A**). Mapping to Hb sequences was possible for 24 peptides using MS/MS spectra to confirm peptide sequences (**Fig. 6B**; green dots). For the remaining putative peptides identified by accurate mass, but for which MS/MS spectra could not be obtained, we assessed whether any peptide isomeric to the putative peptide could be mapped to Hb (**Fig. 6B**; orange dots for peptides mapping to Hb chains and blue dots for peptides that could not be mapped). Overall, ~80% of significantly dysregulated peptides could be mapped to one of the Hb chains, with nearly all increasing in abundance following treatment with MIPS2673 compared to DMSO control. To further validate that the majority of elevated peptides are likely to be Hb-derived, we repeated this same analysis for each of the ~4700 proteins identified in our recent comprehensive proteomic analysis of *P. falciparum*-infected red blood cells.[51] We quantified the number of peptide matches to each protein and then divided by protein length to yield a normalized estimate of the similarity of each protein to our significantly dysregulated peptides. By this measure, Hb chains α, and β were the most highly matched protein compared to the remaining infected red blood cell proteome (**Fig. 6C**; red bars), indicating that MIPS2673 predominantly, but not exclusively, disrupts Hb digestion.

We have recently reported that an inhibitor of *Pf*A-M17 (MIPS2571) also predominantly disrupted metabolism of short haemoglobin-derived peptides, which was a metabolic signature consistent with genetic knockdown of *Pf*A-M17.[11] However, a direct comparison of peptide perturbations induced by MIPS2673 and MIPS2571 (data from Edgar *et al*, 2022) showed clearly distinct peptide profiles. Whilst many peptides accumulated with both inhibitors, the extent of peptide accumulation differed, and a subset of short basic peptides (containing Lys or Arg) were elevated following exposure to MIPS2673, but not the *Pf*A-M17 inhibitor (**Fig. 6A**). Furthermore, the peptide changes observed following treatment with MIPS2673 differ substantially from the peptide changes observed following treatment of *P. falciparum*-infected red blood cells with other potent antimalarials such as artemisinins[55,56] and mefloquine.[57] Those antimalarials induce significant depletion of haemoglobin-derived peptides, in contrast to the accumulation observed with the aminopeptidase inhibitors. Overall, the metabolic profile induced by MIPS2673 is unique, and consistent with specific inhibition of *Pf*A-M1.

Discussion

Here, we report the design of MIPS2673, a hydroxamic acid-based inhibitor that targets both the *P. falciparum* (*Pf*A-M1) and *P. vivax* (*Pv*A-M1) M1 aminopeptidases with excellent selectivity over *Plasmodium* M17 and human M1 homologs. We developed orthogonal mass spectrometry-based chemoproteomics methods based on thermal stability and limited proteolysis to validate, in an unbiased manner, that MIPS2673 engages *Pf*A-M1 in a parasite lysate. This was further supported by untargeted metabolomic profiling that revealed significant accumulation of short peptides in MIPS2673-treated parasites, consistent with *Pf*A-M1 inhibition. MIPS2673 is active against a panel of drug resistant *P. falciparum* strains, including parasites with decreased susceptibility to the current frontline antimalarials, has potential to treat both active disease (asexual blood stage activity) and block parasite transmission (anti-gametocyte activity), and is non-cytotoxic to the human HEK293 cell line. Together, our studies confirm *Plasmodium* M1 alanyl aminopeptidase as the target of MIPS2673 and validate selective inhibition of this enzyme as a promising antimalarial strategy.

The gene encoding *Pf*A-M1 was previously shown to be refractory to knockout and is predicted to be essential for blood stage growth, making it an attractive antimalarial drug target.[12,50] To confirm that MIPS2673 inhibited *Pf*A-M1 in the parasite, we initially developed a streamlined workflow that combined traditional thermal stability proteomics methods with a data-independent acquisition (DIA)-LC-MS/MS approach. Thermal proteome profiling was recently adapted for *P. falciparum* and applied for antimalarial drug target identification using data-dependent acquisition (DDA)-based LC-MS/MS analysis.[45,53,58] Here, protein thermal

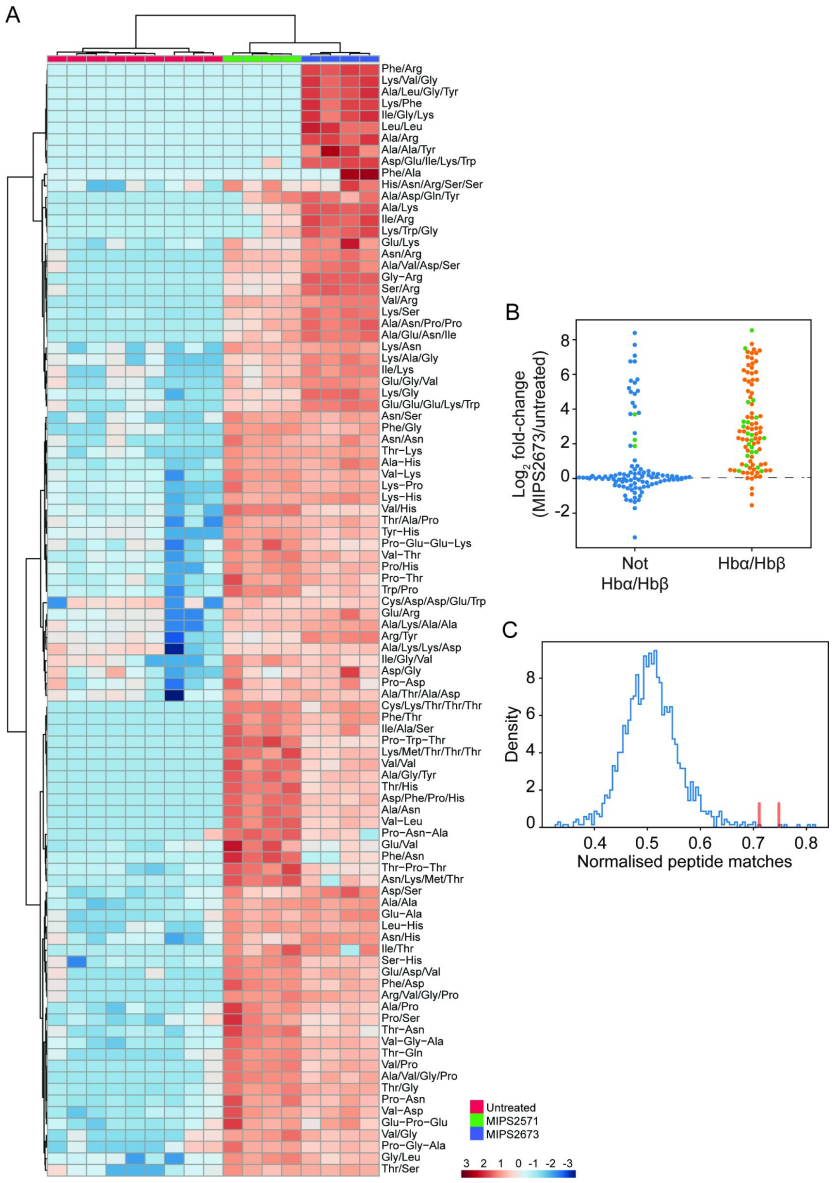

Figure 6

Targeted analysis of significantly dysregulated peptides (p<0.05) following treatment with 1 μM of MIPS2673 (*Pf*A-M1 inhibitor) for 1 h compared to MIPS2571 (*Pf*A-M17 inhibitor) and DMSO control.

(A) Hierarchical clustering of the 97 peptides significantly dysregulated after treatment with MIPS2673 (fold-change >1.5 and p<0.05); 4 biological replicates for MIPS2673 and MIPS2571 (data from Edgar *et al*, 2022)[11] and 9 biological replicates for DMSO control. Vertical clustering displays similarities between samples, while horizontal clusters reveal the relative abundances (median normalized) of the 97 peptides. The color scale bar represents log2 (mean-centered and divided by the standard deviation of each variable) intensity values. Peptides with hyphen (-) notation indicate confirmed sequence by MS/MS. Peptides with slash (/) notation indicate putative amino acid composition (accurate mass), without confirmed sequence order. (B) Differential enrichment of all (201) putatively identified peptides that could (orange dots) or could not (blue dots) be derived from hemoglobin α, and β. Green dots are peptides that have MS/MS spectra and their sequences have been confirmed. (C) Histogram of the sequence similarity of ~4700 proteins present in *P. falciparum* infected red blood cells to the peptides significantly dysregulated by treatment with MIPS2673. Here, sequence similarity is quantified as the number of times a significantly perturbed peptide matches a given protein, normalized by protein length. The Hb chains α, and β are highlighted in red bars.

stabilisation is typically monitored in the presence or absence of compound over a range of temperatures (thermal proteome profiling), or at multiple drug concentrations at a single temperature (isothermal dose response). The extensive samples generated by these approaches require multiplexing with expensive isobaric stable isotope labelling reagents and offline fractionation to minimise sample complexity prior to DDA-LC-MS/MS analysis. Furthermore, DDA-based proteomics is prone to inconsistent peptide detection, which limits the number of proteins that can be reproducibly identified and quantified. In contrast, using DIA analyses in thermal proteome profiling was recently shown to be an effective and economical alternative to traditional DDA-based thermal shift quantitation workflows.[52] DIA-based protein quantification also results in high run-to-run reproducibility and a comprehensive dataset that is not biased towards highly abundant proteins.[43,59] Our DIA-based thermal stability proteomics workflow identified approximately 47% of the detectable *P. falciparum* blood stage proteome,[51] with the undetected proteins primarily comprised of membrane-bound proteins that are not readily extracted with detergent-free buffers required for stability assays of soluble proteins. This proteome coverage is comparable to previously reported DDA thermal proteomics studies of *P. falciparum*,[45,53,58] but our method avoids the need for testing over a wide range of concentrations or temperatures, isobaric tags and offline fractionation steps that increase the time, cost and complexity associated with previously published methods. Since in bacterial and other eukaryotic cellular systems, limited proteolysis coupled with mass spectrometry (LiP-MS) has proven useful for revealing direct drug targets, protein interactions with endogenous metabolites and ligand binding sites at peptide-level resolution,[46,54] we also explored LiP-MS based on DIA-LC-MS/MS as a complementary approach to demonstrate MIPS2673 target engagement in malaria parasites.

Both thermal stability proteomics and LiP-MS strategies support unbiased deconvolution of drug mechanisms on a system-wide scale. Whilst our *in vitro* enzyme assay data demonstrated selective inhibition of recombinant *Pf*A-M1 over *Pf*A-M17 (4-fold), with a *K*i for *Pf*A-M1 inhibition similar to the EC_{50} for killing *P. falciparum in vitro*, this does not rule out inhibition of *Pf*A-M17 or other protein targets within parasites, especially when the EC_{50} concentration approaches the *K*i for *Pf*A-M17 inhibition. Thermal stability proteomics and limited proteolysis coupled with global DIA-LC-MS/MS analysis reproducibly identified *Pf*A-M1 as the target of MIPS2673 from approximately 2,000 detected proteins. This validated our chemoproteomics strategy for detection of ligand-protein interactions in complex proteomes and confirmed the on-target activity and M1-selectivity of MIPS2673. Even at 3x EC_{50}, and concentrations expected to inhibit recombinant *Pf*A-M17, there were no off-targets consistently identified across both thermal stability proteomics and LiP-MS methods, highlighting the importance of using complementary approaches to map drug interactions and discriminate true protein interactors from false positive identifications.

Our structural analysis showed that MIPS2673 acts by chelating the catalytic zinc ion of the *Pf*A-M1 active site, similar to all other inhibitors produced to date.[13,15,19-21,29-33] A strategy targeting the catalytic zinc may present challenges for achieving selectivity over host zinc dependent enzymes, but MIPS2673 demonstrated excellent selectivity over several human M1 homologues, providing rationale for further development of M1 selective inhibitors that present a low risk of host toxicity. Our LiP-MS analysis also supported a zinc-dependent binding mechanism. While other stability-based proteomics methods for drug target identification, such as thermal proteome profiling, map drug-protein interactions by measuring variations in thermal stability of whole proteins, they lack the structural resolution of LiP-MS, which measures local changes in proteolytic susceptibility. Most of the structurally significant *Pf*A-M1 peptides we identified by LiP-MS were within 5 Å of the MIPS2673 binding site determined by X-ray crystallography. The structurally altered peptides identified with LiP-MS included the peptide S_{292}EVIIHPETNYALT$_{305}$, which guards the entrance pathway to the active site and is likely involved in substrate recognition and catalytic competence of the enzyme structure,[60] as well as the peptide L_{449}NLVAVSDFNVGAMENK$_{465}$, which contains the highly conserved GAMEN exopeptidase motif.[30] The GAMEN motif functions to bring substrate to the active site metal for catalysis and contributes hydrogen bonds for ligand binding.[30] Interestingly, we also identified several

structurally significant LiP-MS peptides distal (>5 Å) to this location. Ligands and substrates access the *Pf*A-M1 active site via a long C-terminal channel within domain IV and their migration is orchestrated by several transient states which are stabilized by interactions with specific residues of the domain, including Arg^{969}, Arg^{489}, Lys^{849}, Lys^{907}, Glu^{850}, Asp^{830}, Glu^{572} and Asp^{581}.[61] We identified the structurally significant peptides S_{822}YIVSLPQDR$_{831}$ and R_{898}NTLLSLL$_{905}$ that are located >5 Å from the MIPS2673 binding site at the entrance to the channel cavity. The SYIVSLPQDR and RNTLLSLL peptides contain, or are in very close proximity to, the ASP^{830} and Lys^{907} residues, respectively, which may have a role in regulating recognition and initial passage and migration of ligands into the channel cavity.[61] Together, this demonstrates the potential of LiP-MS not only for unbiased identification of protein targets of drugs, but also for estimating drug binding and interaction sites, which is not possible with many other target deconvolution approaches.

*Pf*A-M1 has been shown to play an essential role in the terminal stages of haemoglobin digestion and the generation of an amino acid pool within the parasite cytosol.[15] Turnover of haemoglobin into oligopeptides and amino acids peaks during the trophozoite stage when *Pf*A-M1 expression and activity is highest. In agreement with *Pf*A-M1 being the target of MIPS2673, we showed that the trophozoite stage coincides with the period that parasites are most susceptible to MIPS2673, and that the growth of MIPS2673-treated parasites becomes stalled at the ring to trophozoite transition. Inhibition of *Pf*A-M1 using an activity-based probe based on the bestatin scaffold resulted in trophozoite stage stalling of parasite growth.[15] However, the activity-based probe also caused digestive vacuole swelling, a phenotype that we did not observe. Digestive vacuole swelling is commonly associated with inhibition of proteases such as the falcipains that are involved in initiating haemoglobin digestion within the parasite digestive vacuole. Since *Pf*A-M1 is a cytoplasmic protein,[28] which is presumed to digest short peptides exported from the digestive vacuole, specific inhibition of this enzyme with MIPS2673 is unlikely to cause digestive vacuole swelling. Instead, the phenotype previously observed with the activity-based probe may be the result of off-target effects. Untargeted metabolomics analysis revealed significant accumulation of short peptides following treatment of parasite cultures with MIPS2673. Many of these accumulated peptides likely originate from haemoglobin as MS/MS and accurate mass isomer analysis shows the sequence of these peptides to be more similar to haemoglobin than other host or parasite proteins. A subset of the dysregulated peptides cannot originate from haemoglobin and may instead derive from other host proteins or the turnover of parasite peptides. While we cannot exclude altered processing of parasite-derived peptides contributing to MIPS2673 activity, starving the parasite of key haemoglobin-derived amino acids appears to be the most likely mechanism leading to parasite death after MIPS2673 treatment.

Several aminopeptidases in addition to *Pf*A-M1 are involved in the terminal stages of peptide processing within malaria parasites. These include the essential aminopeptidases, *Pf*A-M17 and aminopeptidase P (*Pf*APP), and the dispensable enzyme, *Pf*A-M18, all of which share a metal-dependent catalytic mechanism. Although no off-targets were consistently identified in our study, four of the seven putative hits identified in our first LiP-MS experiment were metalloaminopeptidases (*Pf*A-M1, *Pf*A-M17, *Pf*A-M18 and *Pf*APP), with only *Pf*A-M1 reproducibly identified as the primary MIPS2673 target across both LiP-MS experiments. *Pf*A-M18 and *Pf*APP are unlikely to be true off-targets that contribute to the antimalarial mechanism in parasites as we found MIPS2673 is non-inhibitory towards recombinant versions of these enzymes, even at concentrations >120-fold above the EC_{50} for in vitro parasite killing. We found that the median minimum distance for significant LiP peptides from *Pf*A-M17 is closer to the active site than the median distance of all detected peptides (8.56 Å vs 17.47 Å, p=0.045). This suggests that MIPS2673 is interacting close to the *Pf*A-M17 active site. However, *Pf*A-M17 was not stabilised by MIPS2673 in our thermal stability proteomics dataset at 60 °C, a temperature that we previously showed stabilised *Pf*A-M17 when bound to an inhibitor,[11] and specific loss of *Pf*A-M17 function results in multiple membrane bound digestive vacuoles per parasite, a phenotype not observed in parasites treated with MIPS2673. These findings argue against *Pf*A-M17 being a true off-target. Instead,

peptide substrates accumulating due to primary inhibition of *Pf*A-M1 may interact with *Pf*A-M17, leading to structural changes around the enzyme active site that are detected by LiP-MS. Furthermore, distinct peptide profiles for MIPS2673 and a *Pf*A-M17 inhibitor were observed in our metabolomics dataset, with MIPS2673 showing specific accumulation of basic peptides, which agrees with the broad substrate specificity of *Pf*A-M1. In our first LiP-MS experiment we also identified the zinc metalloprotein adenosine deaminase (*Pf*ADA) as a possible MIPS2673 off-target. *Pf*ADA is one of three purine salvage enzymes and catalyses deamination of adenosine to inosine, as well as the conversion of 5'-methylthioadenosine, derived from polyamine biosynthesis, into 5'-methylthioinosine. Investigation of metabolites identified in our metabolomics experiment revealed no significant change in purine or polyamine pathway metabolites, indicating that within 1 h MIPS2673 has no functional impact on these pathways in parasites. Although it is possible that secondary mechanisms, such as impacts to the purine or polyamine pathway, become evident at longer durations of treatment. Interestingly, re-analysis of this dataset from experiment one with a less stringent statistical cut-off (Fisher exact test, uncorrected p<0.05) revealed 47 putative targets (Data S4) that were significantly enriched for metallopeptidase (p=0.022), aminopeptidase (p=2.1E-4), aspartic-type endopeptidase (p=7.34E-3) or threonine-type endopeptidase (p=1.2E-11) gene ontology (GO) terms (**Fig. S6**). Proteins within the metal ion binding gene ontology (GO) term were not significantly enriched (p=0.985) (**Data S5**), confirming that MIPS2673 does not interact indiscriminately with metalloproteins. Whilst this extended list of putative peptidase-related targets may represent plausible secondary targets – either stabilised by MIPS2673 itself or by peptides accumulating due to primary inhibition of *Pf*A-M1 – they do not appear responsible for the antiparasitic activity of MIPS2673, as stabilisation of these additional putative targets was not reproducible across independent experiments, and the relevance of the most significant of these (*Pf*A-M17, *Pf*A-M18, *Pf*APP and *Pf*ADA) is refuted by our thermal stability, metabolomics and recombinant enzyme inhibition data.

Thermal stability proteomics identified *Pf*A-M1 and four other proteins that appeared to be stabilised by MIPS2673. Of these four additional proteins, none were metalloprotein or peptidase off-targets, and only the putative AP2 domain transcription factor (PF3D7_1239200) is a viable drug target based on its predicted essentiality for blood stage growth.[50] This protein is thought to be localised to the parasite nucleus and involved in heterochromatin-associated gene expression.[62] *Pf*A-M1 was previously thought to have nuclear localisation[63] but is now widely accepted to be cytosolic and no function within the parasite nucleus is currently known. With the exception of PF3D7_1239200, it is unlikely that these proteins contribute to MIPS2673 activity in parasites and it is possible that the cell lysis step required to generate a parasite lysate for thermal proteomics (and LiP-MS) introduces artefacts by allowing novel protein interactions or compound access to previously compartmentalised proteins. While the proteins identified individually by thermal stability proteomics and LiP-MS could be MIPS2673-interacting proteins, their lack of consistency across assays suggests that they are likely false discoveries. *Pf*A-M1 was the sole protein reproducibly identified across both unbiased target identification methods, indicating it is the primary target in parasites. However, it should be noted that thermal stability proteomics and LiP-MS rely on complementary stabilisation principles and not all targets will necessarily be amenable to detection by both of these methods. Detecting ligand induced stabilisation of a target will depend on a number of factors, for example, the biophysical properties of the target protein, the experimental design and the depth and coverage of the proteome. Combining multiple complementary approaches will maximise the likelihood of uncovering the complete ligand-protein interaction landscape.

Collectively, we have demonstrated selective targeting of *Plasmodium* M1 alanyl aminopeptidase as an effective antimalarial strategy and validated MIPS2673 as a *Pf*A-M1 inhibitor through unbiased MS-based chemoproteomics. This work provides a basis for continued development of inhibitors against *Plasmodium* M1 alanyl aminopeptidase in an era when new therapeutics with novel mechanisms of action are urgently needed to combat widespread emergence of malaria parasite drug resistance. More broadly, our study demonstrates the power of mass spectrometry-

based techniques to simultaneously probe whole proteomes in an unbiased manner and identify direct drug-protein interactions. The unbiased and orthogonal MS-based proteomics methods described here support investigation of drug mechanisms on a system-wide scale without the need for a specific prior hypothesis about the function of a compound. This makes LiP-MS and thermal stability proteomics ideally suited to reveal the molecular targets of phenotypically active compounds, even for cases where genetic approaches are not tractable. Drug discovery efforts based on phenotypic screens have successfully identified thousands of molecules that kill *Plasmodium* parasites,[64–66] but most of these hits act by unknown mechanisms. Combined, these complementary target identification strategies will provide greater coverage of the druggable proteome and maximise the chance of deconvoluting targets of compounds with uncharacterised modes of action. These strategies can assist in the discovery of new antimalarial drug targets that will facilitate the development of next-generation medicines with novel and diverse mechanisms, ensuring effective treatments for malaria are available in the future.

Methods

Chemistry

Synthetic Materials and Methods. Chemicals and solvents were purchased from standard suppliers and used without further purification. ^{1}H NMR, ^{13}C NMR and ^{19}F NMR spectra were recorded on a Bruker Avance Nanobay III 400MHz Ultrashield Plus spectrometer at 400.13 MHz, 100.61 MHz, and 376.50 MHz, respectively. Chemical shifts (δ) are recorded in parts per million (ppm) with reference to the chemical shift of the deuterated solvent. Unless otherwise stated, samples were dissolved in $CDCl_3$. Coupling constants (*J*) and carbon-fluorine coupling constants (J_{CF}) are recorded in Hz and multiplicities are described by singlet (s), doublet (d), triplet (t), quadruplet (q), broad (br), multiplet (m), doublet of doublets (dd), doublet of triplets (dt). LC-MS was performed using either system A or B. System A: an Agilent 6100 Series Single Quad coupled to an Agilent 1200 Series HPLC using a Phenomenex Luna C8 (2) 50 x 4.6 mm, 5 micron column. The following buffers were used; buffer A: 0.1% formic acid in H_2O; buffer B: 0.1% formic acid in MeCN. Samples were run at a flow rate of 0.5 mL/min for 10 min: 0–4 min 5–100% buffer B in buffer A, 4–7 min 100% buffer B, 7–9 min 100–5% buffer B in buffer A, 9–10 min 5% buffer B in buffer A. Mass spectra were acquired in positive and negative ion mode with a scan range of 100–1000 *m/z*. UV detection was carried out at 254 nm. System B: an Agilent 6120 Series Single Quad coupled to an Agilent 1260 Series HPLC using a Poroshell 120 EC-C18 50 x 3.0 mm, 2.7 micron column. The following buffers were used; buffer A: 0.1% formic acid in H_2O; buffer B: 0.1% formic acid in MeCN. Samples were run at a flow rate of 0.5 mL/min for 5 min; 0–1 min 5% buffer B in buffer A, 1–2.5 min 5– 100% buffer B in buffer A, 2.5–3.8 min 100% buffer B, 3.8–4 min 100–5% buffer B in buffer A, 4–5 min 5% buffer B in buffer A. Mass spectra were acquired in positive and negative ion mode with a scan range of 100–1000 m/z. UV detection was carried out at 214 and 254 nm.

*Methyl 2-(2-hydroxy-2-methylpropanamido)-2-(3',4',5'-trifluoro-[1,1'-biphenyl]-4-yl)acetate (**3**)*. A mixture of methyl 2-amino-2-(4-bromophenyl)acetate (**2**) (400 mg, 1.64 mmol), 2-hydroxy-2-methylpropanoic acid (205 mg, 1.97 mmol), EDCI (1.2 eq) and DMAP (1.3 eq) in DCM (10 mL/mmol of amine) was stirred at room temperature under nitrogen overnight. The mixture was diluted with DCM, washed with 2 M $HCl_{(aq)}$, saturated $NaHCO_{3(aq)}$, then brine. The organic layer was dried over Na_2SO_4, filtered and concentrated under reduced pressure. The product was subsequently reacted with 3,4,5-trifluorophenylboronic acid (347 mg, 1.97 mmol), $Pd(PPh_3)_2Cl_2$ (35 mg, 0.05 mmol), Na_2CO_3 (1 M, 3.3 mL) in THF (9.9 mL) in a sealed microwave vial and heated at 100 °C for 2 h. After cooling, the mixture was diluted with EtOAc (10 mL) and water (10 mL), and the mixture extracted with EtOAc. The organic layer was dried over Na_2SO_4, filtered and concentrated. The crude product was purified by column chromatography to give compound **3** (503 mg, 80%) as a colourless oil. ^{1}H NMR δ 7.73 (br. d, *J* = 7.0 Hz, 1H), 7.53–7.39 (m, 4H), 7.22–7.06 (m, 2H), 5.57 (d, *J* = 7.3 Hz, 1H), 3.76 (s, 3H), 1.50 (s, 3H), 1.44 (s, 3H); ^{19}F NMR δ -133.85 (d, *J* = 20.5 Hz), -162.09 (dd, *J* =

20.5 Hz); ^{13}C NMR δ 175.9, 171.1, 151.6 (ddd, J_{CF} = 250.3/10.2/4.6 Hz), 141.2–138.0 (m, 2C), 136.9, 136.8–136.5 (m), 128.1, 127.7, 111.6–110.9 (m), 73.8, 56.1, 53.1, 28.0, 27.9; LC-MS t_R: 3.4 min, *m/z* 381.9 $[MH]^+$.

*2-Hydroxy-N-(2-(hydroxyamino)-2-oxo-1-(3',4',5'-trifluoro-[1,1'-biphenyl]-4-yl)ethyl)-2-methylpropanamide [MIPS2673 (**4**)]*. Methyl 2-(2-hydroxy-2-methylpropanamido)-2-(3',4',5'-trifluoro-[1,1'-biphenyl]-4-yl)acetate (**3**) (100 mg, 0.26 mmol) was dissolved in anhydrous MeOH (5 mL/mmol of ester) at room temperature. $NH_2OH.HCl$ (4.0 eq) was added followed by KOH (5M in anhydrous MeOH, 5.0 eq). The mixture was stirred at room temperature overnight and monitored by LC-MS analysis. The mixtures were directly dry-loaded on to Isolute HM-N® (Biotage), before purification by FCC. The desired hydroxamic acid 3 was obtained as white solid (40 mg, 40% yield). ^{1}H NMR (DMSO-d_6) δ 11.13 (s, 1H), 9.15 (s, 1H), 8.07 (d, *J* = 8.1 Hz, 1H), 7.78–7.63 (m, 4H), 7.46 (d, *J* = 8.3 Hz, 2H), 5.74 (s, 1H), 5.29 (d, *J* = 8.1 Hz, 1H), 1.26 (s, 3H), 1.23 (s, 3H); ^{19}F NMR (DMSO-d_6) δ -134.91 (d, *J* = 21.7 Hz), -163.45 (dd, *J* = 21.8 Hz). ^{13}C NMR (DMSO-d_6) δ 176.2, 166.4, 150.9 (ddd, J_{CF} = 246.8/9.8/4.3 Hz), 139.5, 140.2–137.1 (m), 136.9–136.4 (m, 2C), 127.3, 127.2, 111.8–110.9 (m), 72.5, 53.2, 27.8, 27.6; *m/z* HRMS (TOF ES$^+$) $C_{18}H_{18}F_3N_2O_4$ $[MH]^+$ calcd 383.1213; found 383.1214; LC-MS t_R: 3.2 min; HPLC t_R: 7.7 min, >99%.

Routine parasite culture

P. falciparum parasites (3D7 line) were cultured continuously in O+ human red blood cells (Australian Red Cross Blood Service) at 2-4% haematocrit using standard methods,[67] with minor modifications.[55] Briefly, cultures were maintained at 37 °C under defined atmospheric conditions (94% N_2, 5% CO_2, and 1% O_2) in RPMI 1640 medium supplemented with 0.5% Albumax II (Gibco, Australia), HEPES (5.94 g/L), hypoxanthine (50 mg/L) and sodium bicarbonate (2.1 g/L). Parasites were synchronised using multiple rounds of sorbitol lysis[68] and monitored at least every 48 h by Giemsa staining of methanol-fixed blood smears.

Parasite material for thermal stability and limited proteolysis experiments was obtained from cultures synchronised to 30-38 h post invasion. Parasites were isolated from red blood cells via hypotonic lysis to avoid the use of solubilising molecules such as saponin. Briefly, infected red blood cells were magnetically purified and incubated with 10 mL of hypotonic lysis buffer (150 mM ammonium chloride, 10 mM potassium bicarbonate, 1 mM EDTA in Milli-Q water) for 5 min at 4 °C. Following hypotonic lysis, the intact parasite pellets were washed three times in PBS and stored at -80°C until whole proteome preparation.

Whole proteome preparation

Parasite pellets were resuspended in 1-2 mL of cold 100 mM HEPES buffer (pH 8.1) and subjected to freeze-thaw lysis by cycling at 2-3 min intervals between dry ice and a 35°C heat block. Cells used for limited proteolysis also underwent mechanical shearing after freeze-thaw lysis by passing the thawed suspension through a 26-gauge (10-20x) and then a 30.5-gauge needle (10-20x). The resulting lysates were centrifuged to remove cell debris (20,000 *g* for 20 min at 4 °C), the supernatants collected and combined to create one pooled parasite lysate. For thermal stability experiments, the cell debris obtained after centrifugation underwent two additional cycles of freeze-thaw and the collected supernatants were added to the pooled lysate. All remaining steps were performed at 4 °C. The protein concentration of the resulting lysate was determined using the Pierce bicinchoninic acid (BCA) protein assay kit (Thermofisher Scientific).

Lysate treatment for thermal stability proteomics and MS analysis

The pooled lysate was equally separated to achieve at least three incubations (technical replicates) per condition. The parasite lysates were incubated with 1 µM or 4 µM of MIPS2673 or vehicle (DMSO) for 3 min at room temperature, followed by thermal challenge at 60 °C for 5 min. Each sample was incubated at room temperature for a further 3 min prior to being returned to ice. The

denatured protein was removed via ultracentrifugation at 100,000 *g* for 20 min (4 °C) in a Beckman Coulter Optima XE-90 – IVD ultracentrifuge with a 42.2 Ti rotor. The protein concentration in the soluble fraction was determined using a BCA assay. Samples were then reduced and alkylated at 95 °C for 5 min using 10 mM tris(2-carboxyethyl)phosphine hydrochloride (TCEP) and 40 mM iodoacetamide (40 mM final concentration), respectively. Each sample was digested overnight with MS-grade trypsin (1:50; Promega) at 37 °C while shaking. The following day, trypsin activity was quenched using 5% formic acid (FA) and samples were subjected to desalting using in-house-generated StageTips, as described previously.[69] The samples were then dried and resuspended in 12 µL of 2% (v/v) acetonitrile (ACN) and 0.1% (v/v) FA containing indexed retention time (iRT) peptides (Biognosys) for LC-MS/MS analysis.

Lysate treatment for limited proteolysis and MS analysis

An equivalent volume of protein lysate was aliquoted from a lysate pool for a minimum of three independent incubations per condition and incubated with MIPS2673 (0.04 µM to 40 µM) or vehicle (DMSO) at room temperature for 10 min. Proteinase K from *Tritirachium album* (Sigma Aldrich) was added to all of the reactions at a 1:100 ratio of enzyme to protein and incubated at room temperature for 4 min. The digestion reactions were stopped by heating samples to 98°C for 1 min, followed by addition of an equal volume of 10% sodium deoxycholate (Sigma Aldrich) to achieve a final concentration of 5%. Samples were incubated for a further 15 min at 98°C. These samples were then removed from the heat and subjected to complete digestion under denaturing conditions.

Samples were reduced and alkylated for 10 min at 95 °C with 10 mM TCEP and 40 mM chloroacetamide, respectively. Subsequently, samples were digested with Trypsin/LysC (1:100 enzyme to substrate ratio) for 16 h at 37 °C while shaking. Deoxycholate was precipitated by addition of formic acid to a final concentration of 1.5% and centrifuged at 16,000 g for 10 min. After transferring the supernatant to a new tube an equal volume of FA was added again and the centrifugation repeated. Digests were desalted using in-house-generated StageTips[69] and after drying resuspended in 12 µL of 2% (v/v) ACN and 0.1% (v/v) FA containing iRT peptides (Biognosys) for LC-MS/MS analysis.

LC-MS/MS acquisition for proteomics

LC-MS/MS was carried out using data-independent acquisition mode on a Q-Exactive HF mass spectrometer (Thermo Scientific) as described previously.[51] Briefly, samples were loaded at a flow rate of 15 µL/min onto a reversed-phase trap column (100 µm x 2 cm), Acclaim PepMap media (Dionex), maintained at a temperature of 40 °C. Peptides were eluted from the trap column at a flow rate of 0.25 µL/min through a reversed-phase capillary column (75 µm x 50 cm) (LC Packings, Dionex). The HPLC gradient was 158 min and gradually reached 30% ACN after 123 min, 34% ACN after 126 min, 79% ACN after 131 min and 2% after 138 min for a further 20 min. The mass spectrometer was operated in a data-independent mode with a 43-fixed-window setup of 18 *m/z* effective precursor isolation over the m/z range of 364-988 Da. Full scan was performed at 60,000 resolution (AGC target of 3e[6] and maximum injection time of 54 ms) with fragmentation resolution at 15,000 (AGC target of 2e[5], maximum injection time of 22 ms, normalized collision energy of 27.0).

Data analysis for thermal stability proteomics experiments

Raw files were processed using Spectronaut™ 13.0 against an in-house generated P. falciparum infected red blood cell spectral library as described previously.[51] The consensus library contained 42,245 peptides corresponding to 4,421 protein groups. For processing, raw files were loaded and Spectronaut calculated the ideal mass tolerances for data extraction and scoring based on its extensive mass calibration with a correction factor of 1. Both at precursor and fragment level, the highest data-point within the selected *m/z* tolerance was chosen. Identification of

peptides against the library was based on default Spectronaut settings (Manual for Spectronaut 13.0, available on Biognosis website). Briefly, precursor Qvalue Cut-off and Protein Qvalue Cut-off were as per default at 1%, therefore only those that passed the cut-off were considered as identified and used for subsequent processing. Retention time prediction type was set to dynamic iRT. Interference correction was on MS2 level. For quantification, the interference correction was activated and a cross run normalisation was performed using the total peak area as the normalisation base with a significance level of 0.01.

Significantly stabilised proteins were determined by first calculating the fold-change between the MIPS2673 (1 μM and 4 μM conditions) and vehicle-treated samples for each experiment. Statistical significance of the change in protein abundance was determined by a Welch's t-test. Proteins that were significantly stabilised (fold-change >1.2, $p<0.05$) at both MIPS2673 concentrations in multiple experiments were considered putative targets. The data were plotted using paired volcano plots, whereby fold-change in protein abundance was plotted as a function of statistical significance for multiple conditions or experiments to visualise commonly stabilised proteins.

Data analysis for limited proteolysis experiments

For limited proteolysis experiments, raw data files were processed using Spectronaut^{TM} 13.0 as described above, except a limited proteolysis-specific *P. falciparum* infected red blood cell spectral library was used. The in-house generated library contained 85,039 peptides corresponding to 4,681 protein groups.

All limited proteolysis datasets were analysed at the modified peptide sequence level. The datasets were first analysed for differentially abundant peptides between MIPS2673 and vehicle by filtering based upon relative peptide abundance (absolute fold-change >1.5) and statistical significance ($q<0.01$). Within independent experiments, peptides meeting these thresholds at each drug concentration were considered significant. To filter and prioritise possible protein targets, a one-sided Fisher exact test was used to determine whether, based on the total number of peptides detected for each protein in the dataset, the number of significant LiP peptides identified for each protein was greater than would be expected by chance. Resulting p-values were adjusted for multiple testing using the Bonferroni method. Proteins passing the Bonferroni corrected statistical cut-off were considered putative targets. Proteins that did not pass the stringent Bonferroni corrected statistical cut-off, but were statistically significant ($p<0.05$) were considered lower confidence targets.

The position of drug binding using the centre of mass and distance measurements were performed using PyMol 2.5.1 (Schrodinger). Distance measurement analyses considered only peptides detected in both LiP-MS experiments. For the MIPS2673-*Pf*A-M1 interaction, we mapped peptides to our experimentally determined *Pf*A-M1 structure with MIPS2673 bound (PDB: 8SLO). Significant LiP peptides were defined as peptides that passed the relative abundance (absolute fold-change >1.5), statistical significance ($q<0.01$) and proteolytic peptide pattern (i.e. increased fully tryptic or decreased half tryptic) filters at all concentrations tested in both experiments. For other putative MIPS2673 interacting proteins identified by thermal stability proteomics and by LiP-MS in experiment one, only one significant LiP peptide was identified (YSPSFMSFK from *Pf*ADA) using the above criteria to define significant LiP peptides. Thus, for distance measurement analyses of these other putative MIPS2673 interacting proteins we applied a less stringent rule for defining significant LiP peptides, namely, any peptide that passed the relative abundance (absolute fold-change >1.5), statistical significance ($q<0.01$) and proteolytic peptide pattern (i.e. increased fully tryptic or decreased half tryptic) filters at any concentration in both experiments. The active site metal ion (*Pf*ADA PDB: 6II7, *Pf*A-M17 PDB: 7RIE, *Pf*APP PDB: 5JR6) or ligand (*Pf*MIF PDB: 4P7S, TRXR1 PDB: 2ZZC) were used as a reference point for minimum distance measurements. For RAB39A, which is not a metalloprotein and where no ligand-bound structure is available, the GTP binding site residues were used (AlphaFold: AF-Q14964-F1). The putative *Pf*ApiAP2 transcription factor, PF3D7_1239200, was excluded from this analysis as no protein structure is available and

the AlphaFold predicted structure is of very low quality (pLDDT score 36.67). No peptides met the significance criteria for *Pf*A-M18 and the conserved parasite proteins, PF3D7_1026000 and PF3D7_0604300.

To reveal in an unbiased way whether any protein functions are overrepresented in the expanded list of candidate targets from the experiment one dataset, this list was tested for functional enrichments using the *top*GO R-package.[70] All proteins with an uncorrected p<0.05 were tested against a background of proteins for which abundance was measured. PlasmoDB GO terms were used for GO term mapping. We tested for enrichment in molecular function GO terms with the Fisher exact test using the weight-algorithm in topGO.[71] All terms with a p-value less than 0.05 were considered significant. GO terms represented by fewer than five proteins in the background dataset were excluded from the analysis.

Enzyme assays

Inhibition of aminopeptidase activity assays were performed against nine aminopeptidases: the M1 alanyl and M17 leucyl aminopeptidases from *Plasmodium falciparum* (*Pf*A-M1; *Pf*A-M17) and *Plasmodium vivax* (*Pv*A-M1; *Pv*A-M17), the M18 aspartyl and aminopeptidase P aminopeptidases from *Plasmodium falciparum* (*Pf*A-M18; *Pf*APP) and three human M1 homologues: LTA4H (OriGene TP307617), ERAP1 (OriGene TP314469) and ERAP2 (Creative BioMart ERAP2-304H). The *Plasmodium* enzymes were produced recombinantly as described previously[30,34,72-74] and the human recombinant enzymes were purchased from commercial suppliers as indicated.

The ability of MIPS2673 to inhibit aminopeptidase activity was assessed by fluorescence assays using fluorogenic substrates *L*-Leucine-7-amido-4-methylcoumarin hydrochloride (H-Leu-NHMec, 20 μM for *Pf*A-M1, 40 μM for *Pv*A-M1 and 100 μM for ERAP1 and ERAP2) for all enzymes except LTA4H that was assessed using *L*-Alanine-7-amido-4-methylcoumarin hydrochloride (H-Ala-NHMec, 20 μM) and *Pf*APP that was assessed using Lys(Abz)-Pro-Pro-NA (PPpNA, 10 μM).[20] Aminopeptidase activity of *Pf*-M18 was measured by an absorbance assay using the substrate L-glutamic acid g-(4-nitroanilide) (L-Glu-pNA, 100 μM).[74] All assays were performed at pH 8.0. The concentration of substrate in the assay was held constant for each enzyme and ranged from 10–100 μM depending on the enzyme. Reactions were measured at 37 °C in white 384–well plates in a total volume of 50 μL using a spectrofluorimeter (BMG FLUOstar) with excitation at 355 nm and emission at 460 nm for the fluorescence assays or excitation at 405 nm for the absorbance assays. The fluorescence or absorbance signal was continuously monitored until a final steady state velocity, *v*, was obtained. Inhibition constants were calculated in biological triplicate from three different protein preparations. For determination of the apparent Morrison inhibition constant (denoted here as K_i), enzymes were pre-incubated in 100 mM Tris–HCl, pH 8.0 (supplemented with 1 mM $CoCl_2$ for M17 aminopeptidases) and inhibitor added 20 min prior to the addition of substrate. Substrate concentrations were selected to allow sensitive detection of enzyme activity while not exceeding the K_m for each enzyme. A compound concentration range was selected to obtain a complete inhibition curve (0% – 100 %) in biological triplicate. Where possible, the K_i values were calculated by plotting the initial rates versus inhibitor concentration, and fitting to the Morrison equation for tight-binding inhibitors in GraphPad Prism (non-linear regression method). Where a K_i could not be calculated (ERAP1), the percentage inhibition was calculated assuming 100% activity in the absence of compound.

Structural biology

*Pf*A-M1 was co-crystallized with MIPS2673 by the hanging-drop method using previously established protocols.[30] Purified protein was concentrated to 5.0 mg/mL and mixed with MIPS2673 to a final ligand concentration of 1 mM. Crystals grew in 20−30% poly(ethylene glycol) (PEG)8000, 0.1 M Tris pH 7.5−8.5, 0.2 M $MgCl_2$, 10% glycerol. Co-crystals were subjected to an additional overnight compound soak before being snap-frozen in liquid nitrogen. Data were collected at 100 K using synchrotron radiation at the Australian Synchrotron beamlines 3BM1.[75]

Data were processed using XDS,[76] and Aimless[77] as part of the CCP4i program suite.[78] The structures were solved by molecular replacement in Phaser[79] using the structure of unliganded *Pf*A-M1 coordinates (RCSB ID 3EBG) as the search models. The structures were refined using Phenix,[80] with 5% of reflections set aside for calculation of R_{free}. Between refinement cycles, the protein structure, solvent, and inhibitors were manually built into $2F_o - F_c$ and $F_o - F_c$ electron density maps using COOT,[81,82] with restraint files generated by Phenix where necessary. The data collection and refinement statistics can be found in Supplemental Information (Table S5). The coordinates and structure factors are available from the Protein Data Bank with PDB Accession codes: 8SLO.pdb (*Pf*A-M1-MIPS2673).

Determination of compound EC_{50} against 3D7 *P. falciparum* parasites

Parasite viability assay was performed as previously described.[11] Synchronized ring stage *P. falciparum* 3D7 parasites were cultured in 96-well U-bottom plates at 0.5% parasitemia and 2% haematocrit, to which 50 µL of serially diluted MIPS2673 or artesunate was added. After 72 h plates were placed at -80ºC before being analysed in buffer containing 20 mM Tris pH 7.5, 5 mM EDTA, 0.008% saponin (w/v) and 0.008% Triton x-100 (v/v)[83] containing 0.2 µL/mL SYBR Green I Nucleic Acid Gel Stain (10,000x in DMSO; ThermoFisher). After 1 h incubation, fluorescence intensity was read on a Glomax® Explorer Fully Loaded plate reader (Promega) at emission wavelengths of 500-550 nm and an excitation wavelength of 475 nm. Uninfected RBCs and parasites treated with DMSO were used to normalize fluorescence. Data from 4 biological replicates performed in triplicate were plotted as 4-parameter log dose nonlinear regression analysis with a sigmoidal dose-response curve fitted using GraphPad Prism 9 to generate EC_{50} values, with error bars representative of the SEM.

EC_{50} determination against drug resistant field isolates and laboratory selected *P. falciparum* parasites

In vitro testing was performed with a modified [^{3}H]-hypoxanthine incorporation assay, as previously reported.[84]

Parasite killing rate assay

Assay was performed as previously described.[11] Synchronized ring or trophozoite *P. falciparum* 3D7 parasites were cultured in the presence of 10x the EC_{50} of MIPS2673 or artesunate for either 24 or 48 h. Media containing compound was replenished at 24 h for 48 h assays. After incubation, RBCs were thoroughly washed to remove the compound and cultures were diluted 1/3 with fresh media and further grown for 48 h before being placed at -80 ºC. Cultures were thawed and analyzed using SYBR Green I assay as described above. Parasite viability was determined as a percentage of DMSO-treated parasites cultured alongside compound treated parasites. Artesunate was used as a comparison of the parasite killing rate, and experiments were performed in 4 biological replicates

Gametocyte activity assay

Viability assays were performed as previously described[85–87] against *Pf*NF54-s16-GFP early (I-III); late (IV-V) and mature (V) stage gametocytes. Gametocytes were assessed at early stage (day 2), late stage (day 8) and mature (day 12). Compounds diluted in 4% DMSO were transferred into 384-well imaging plates; gametocytes at various stages added, and plates incubated for 72 h in 5% CO_2, 5% O_2 and 60% humidity at 37 °C. After 72 h incubation, 5 µL of MitoTracker Red CMH2XRos in phosphate buffered saline (PBS) added per well and plates incubated overnight. Image acquisition and analysis was undertaken on the Opera QEHS micro-plate confocal imaging system. An Acapella based script using the MTR fluorescent signal and the GFP designated object quantifying

viable stage dependent parasite morphology identified gametocytes. Gametocyte viability was calculated as a percentage of the positive (5 µM puromycin) and negative (0.4% DMSO) controls. EC_{50} values were calculated using a 4-parameter log dose, non-linear regression analysis, with sigmoidal dose response (variable slope) curve fit using Graph Pad Prism (ver 4.0). No constraints were used in the curve fit. Chloroquine, artesunate, pyronaridine, pyrimethamine, dihydroartemisinin and methylene blue were analysed in parallel as reference compounds. Experiments were completed in duplicate for 2 or 3 biological replicates.

HEK293 cytotoxicity assay

To assess the cytotoxicity of MIPS2673 against mammalian cells, an established and well validated metabolic assay for HEK293 cells was used.[88] In brief, HEK293 cells were maintained in DMEM medium supplemented with 10% fetal bovine serum. Compound testing was undertaken in tissue culture-treated 384-well plates incubated for 72 h at 37 ° and 5% CO_2. The media was then removed and replaced with resazurin (final concentration 44 µM). After an additional 6 h incubation, total fluorescence was measured using an Envision plate reader (Perkin Elmer) (excitation/emission: 530 nm/595 nm).

Metabolomics

P. falciparum 3D7 cultures that underwent double sorbitol synchronisation were incubated for a further 28–42 h to achieve the desired trophozoite stage (28 hours post invasion (h.p.i)). Infected RBC cultures at 6% parasitaemia and 2% haematocrit (2 x 10^8 cells in total) were treated with 3 x the EC_{50} of MIPS2673 (1 µM) or an equivalent volume of DMSO (negative control) for 1 h, after which metabolites were extracted. Following incubation, all samples were centrifuged at 650 g for 3 min, supernatants were removed, and pellets were washed in 1 mL of ice-cold PBS. Samples were again centrifuged at 650 g for 3 min to remove all of the PBS and the pellets were resuspended in 150 µL of ice-cold extraction buffer (100% methanol). Samples were then incubated on an automatic vortex mixer for 1 h at 4 °C before being centrifuged at 21,000 g for 10 min. Supernatant was collected and 100 µL was stored at –80 °C until further analysis and 10 µL from each sample was pooled to serve as a quality control (QC) sample. Liquid chromatography coupled to mass spectrometry (LC-MS) analysis and data processing were as previously described.[11]

Kinetic solubility estimation

Kinetic solubility was estimated using nephelometry (Sol_{pH}) according to the method of Bevan and Lloyd.[89] Briefly, the compound in DMSO was spiked into either pH 6.5 phosphate buffer or 0.01 M HCl (approximately pH 2) with the final DMSO concentration being 1%. After 30 min had elapsed, samples were then analysed via nephelometry to determine a solubility range.

Acknowledgements

The authors wish to thank and acknowledge the Australian Red Cross LifeBlood for the provision of fresh red blood cells, without which antimalarial testing could not have been performed. The Centre for Drug Candidate Optimisation (CDCO, Monash University) is acknowledged for providing the solubility data. The CDCO is partially supported by the Monash University Technology Research Platform network and Therapeutic Innovation Australia (TIA) through the Australian Government National Collaborative Research Infrastructure Strategy (NCRIS) program. We thank the following colleague for support with the *Plasmodium falciparum* strain panel assays: Sibylle Sax, Swiss Tropical and Public Health Institute, Switzerland. We thank the Monash Proteomics and Metabolomics Facility for technical support. S.D. was supported by a NHMRC Dora Lush Biomedical Postgraduate Scholarship (APP1150359), Griffith University DVCR Postgraduate Top-up

Scholarship and a Discovery Biology Top-up Scholarship. V.M.A acknowledges Medicines for Malaria Venture for continued financial support. Funding was provided by an NHMRC Synergy Grant for the Antimalarial Synergy Team #1185354.

Declarations

Significance

Drug resistance now threatens all existing treatments for malaria, the world's most lethal parasitic disease of humans. As a result, there is an urgent need for new antimalarial drug candidates that act via novel pathways and have a high barrier for resistance. It is therefore important to understand the mechanism of action for emerging antimalarials. However, target deconvolution is a major bottleneck for new drug development for malaria, particularly when genetic approaches for target identification are not possible. Mass spectrometry-based chemoproteomics has emerged as a powerful alternative strategy to deconvolute drug protein targets in a proteome-wide and unbiased manner. To this end, we report a novel promising antimalarial compound targeting M1 alanyl aminopeptidase (*Pf*A-M1) in the malaria parasite, and validate this target by combining biochemical assays on recombinant enzymes, with metabolomics, thermal stability chemoproteomics and a novel drug target deconvolution strategy for *Plasmodium falciparum*: limited proteolysis coupled mass spectrometry (LiP-MS). LiP-MS uses mass spectrometry to detect proteolytic stabilisation of proteins in a parasite lysate due to ligand binding. LiP-MS also estimated the binding site of MIPS2673 on *Pf*A-M1 to within ~5 Å of that determined by X-ray crystallography, highlighting the value of this approach in resolving both the molecular target and binding site of drugs. Implementing LiP-MS in *P. falciparum* expands the drug target deconvolution toolbox for malaria drug discovery. Our studies chemically validated selective targeting of *Plasmodium* M1 alanyl aminopeptidase as a potential multi-stage and cross-species strategy for the treatment of malaria and demonstrated the value of combining multiple orthogonal mechanism of action studies for target deconvolution. This combination of methods provides a validated workflow to help uncover the targets of other promising antimalarial candidates in the pipeline.

Author contributions

Conceptualization, C.G., M.P.C., T.F.dK-W., P.J.S., S.M., and D.J.C.; Formal Analysis, C.G., M.P.C., G.S., R.C.S.E., T.R.M., C.T.W., N.D., C.A.M., S.D., S.W., and S.M.; Investigation, C.G., M.P.C., G.S., R.C.S.E., T.R.M., C.T.W., N.D., N.B.V., N.A.C., and S.D., Resources, S.W., V.M.A., T.F.dK-W., P.J.S., S.M., and D.J.C.; Data Curation, C.G., M.P.C., G.S., R.C.S.E., T.R.M., C.T.W., N.D., N.B.V., S.D., and S.W.; Writing – Original Draft, C.G., G.S., P.J.S., S.M., and D.J.C.; Writing – Review & Editing, C.G., M.P.C., G.S., R.C.S.E., C.T.W., N.B.V., C.A.M., S.W., S.M.D., V.M.A., T.F.dK-W., P.J.S., S.M., and D.J.C.; Visualisation, C.G., M.P.C., G.S., R.C.S.E., C.A.M., P.J.S., and S.M.; Supervision, S.M.D., V.M.A., T.F.dK-W., P.J.S., S.M., and D.J.C.; Project Administration, C.G., T.F.dK-W., P.J.S., S.M., and D.J.C; Funding Acquisition, T.F.dK-W., P.J.S., S.M., and D.J.C.

Data and code availability

The mass spectrometry proteomics data have been deposited to the ProteomeXchange Consortium via the PRIDE[90] partner repository (*https://www.ebi.ac.uk/pride/archive/*) with the dataset identifier PXD044125.

The mass spectrometry metabolomics data is *available at the NIH Common Fund's National Metabolomics Data Repository (NMDR) website, the Metabolomics Workbench, https://www .metabolomicsworkbench.org where it has been assigned Project ID (ST002792). The data can be accessed directly via it's Project DOI: 10.21228/M8SQ7X. This work is supported by Metabolomics*

Workbench/National Metabolomics Data Repository (NMDR) (grant# U2C-DK119886), Common Fund Data Ecosystem (CFDE) (grant# 3OT2OD030544) and Metabolomics Consortium Coordinating Center (M3C) (grant# 1U2C-DK119889)

Structural data has been deposited with PDB with the identifier 8SLO.

This paper does not report original code.

Any additional information required to reanalyze the data reported in this paper is available from the lead contact upon request.

Supplemental Information

Supplemental Fig. S1

Antimalarial potency of the clinically used artemisinin derivative, artesunate. Related to Fig. 1.

Sensitivity to artesunate exposure (72 h) for *P. falciparum* 3D7 parasites. Artesunate activity was tested alongside MIPS2673 as a reference compound with known antimalarial activity. Parasite growth was determined relative to a no-drug control by SYBR Green I assay. The EC_{50} value was calculated from 4 biological replicates performed in technical triplicate and the data plotted as the mean ± standard error of the mean.

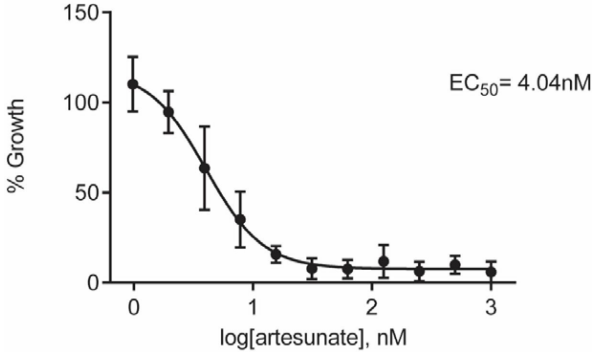

Supplemental Fig. S2

Individual thermal stabilisation profile of *Pf*A-M17 leucyl aminopeptidase after *P. falciparum* lysate treatment with MIPS2673. Related to Fig. 3.

Abundance of *Pf*A-M17 leucyl aminopeptidase from *P. falciparum* lysates in the absence and presence of MIPS2673 after a 60 °C thermal challenge. *Pf*A-M17 was not stabilised by MIPS2673 after a 60 °C thermal challenge ($p>0.05$). Error bars indicate SD (n = 4 independent lysate incubations per condition in each independent experiment).

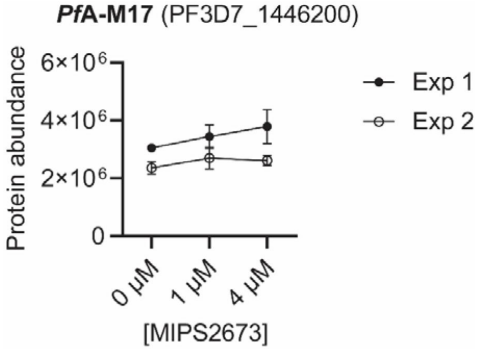

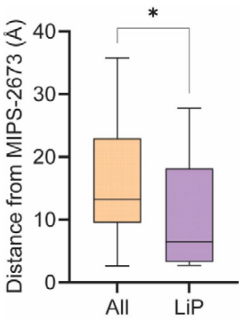

Supplemental Fig. S3

Minimum distance of significant LiP-MS or all other *Pf*A-M1 peptides from bound MIPS2673. Related to Fig. 5.

Among the 108 *Pf*A-M1 peptides commonly identified across both LiP-MS experiments, nine peptides were significantly dysregulated in the presence of MIPS2673 at all concentrations tested. The atoms of these LiP peptides were used to measure the distribution of distances to bound MIPS2673 compared to all detected *Pf*A-M1 peptides. * $p < 0.05$, Mann-Whitney test.

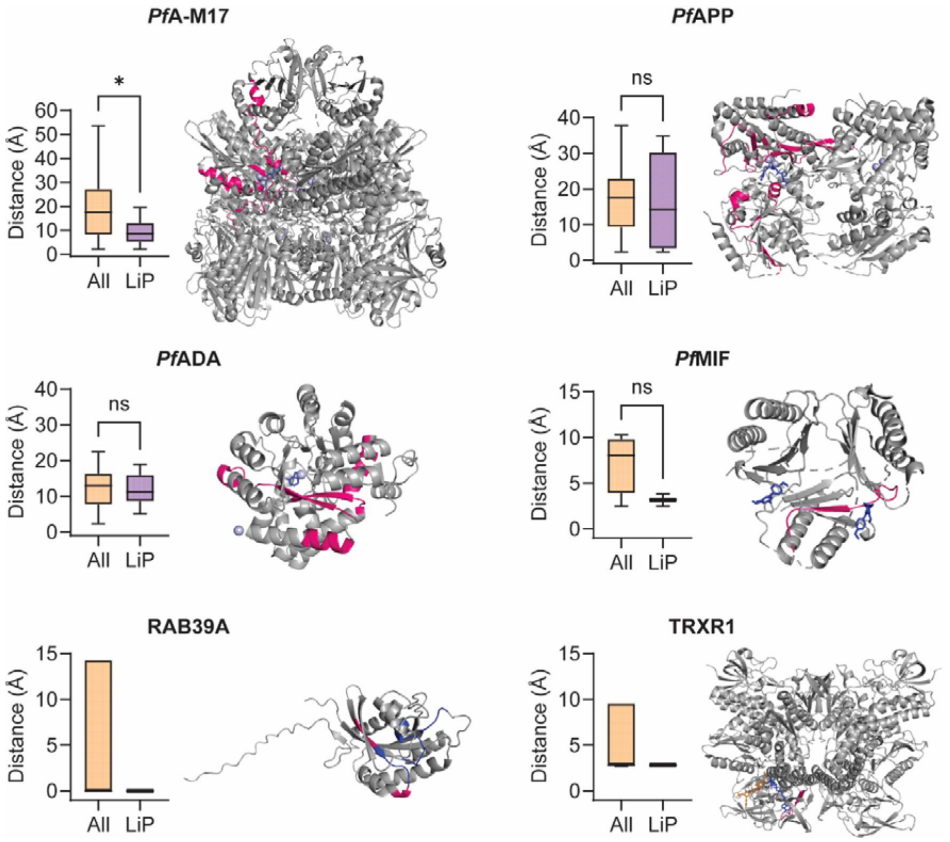

Supplemental Fig. S4

Minimum distance measurements and mapping of significant LiP-MS peptides to structures of other putative MIPS2673-interacting proteins. Related to Fig. 5.

Distance measurement analyses were performed for other putative MIPS2673-interacting proteins identified with thermal stability proteomics and LiP-MS (experiment one) where a protein structure was available and significant LiP-MS peptides were identified. Only peptides detected in both LiP-MS experiments were considered for analysis. Significant LiP peptides were defined as any peptide that passed the relative abundance (absolute fold-change >1.5), statistical significance (q<0.01) and proteolytic peptide pattern (i.e. increased fully tryptic or decreased half tryptic) filters at any concentration in both LiP-MS experiments. For the metalloproteins *Pf*A-M17, *Pf*APP and *Pf*ADA (PDB: 7RIE, 5JR6 and 6II7, respectively) the active site metal ions were used as a reference point for minimum distance measurements. For *Pf*MIF (PDB: 4P7S), the bound ligand 20K, and TRXR1 (PDB: 2ZZC), the bound ligands FAD and NADP, were used for minimum distance measurements. For RAB39A, which is not a metalloprotein and where no ligand-bound structure is available, the GTP binding site residues (blue) were used (AlphaFold: AF-Q14964-F1). Significant LiP-MS peptides are in pink, metal ions are in light blue and ligands are in dark blue or orange (NADP only). Peptide mapping for multimeric proteins was performed for one chain only (chain A for *Pf*A-M17, *Pf*APP and TRXR1 and chain B for *Pf*MIF). The putative *Pf*ApiAP2 transcription factor, PF3D7_1239200, was excluded as no protein structure is available and the AlphaFold predicted structure is of very low quality (pLDDT score 36.67). No peptides met the significance criteria for *Pf*A-M18 and the conserved parasite proteins, PF3D7_1026000 and PF3D7_0604300. * p < 0.05, Mann-Whitney test. For RAB39A and TRXR1, where only one significant LiP-MS peptide was identified per protein, statistical significance was not determined

Supplemental Fig. S5

Untargeted metabolomics analysis of 3D7 parasites treated with 1 μM of MIPS2673. Related to Fig. 6.

Heatmap analysis of peak intensities of all putative metabolites for each condition; 1 μM of MIPS2673 for 1 h and DMSO control (untreated). Data is shown from 4-9 biological replicates, red, blue and yellow indicates increase, decrease and no change, respectively in the relative abundance of putative metabolites identified.

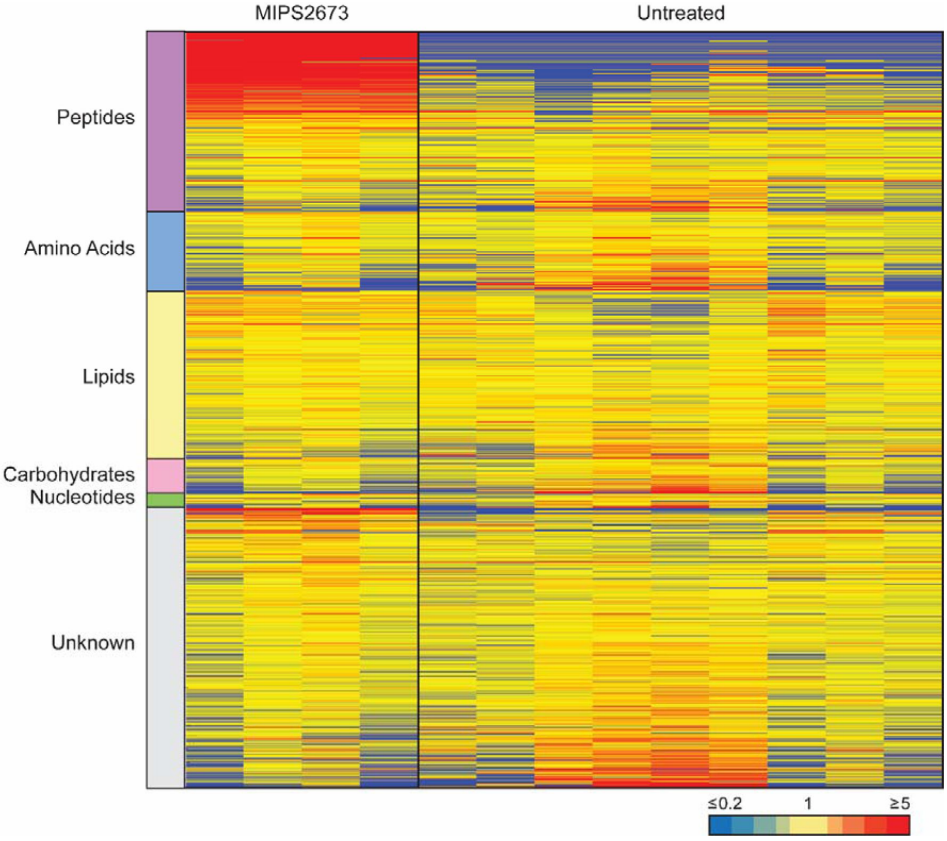

Supplemental Fig. S6

Molecular function GO enrichment analysis of the MIPS2673 experiment one LiP-MS dataset. Related to Fig. 4.

Fold enrichment (left) and significance (right) of GO molecular functions enriched among the expanded list of candidate MIPS2673 targets identified in the first LiP-MS experiment. All proteins with an uncorrected p<0.05 were tested against a background of proteins for which abundance was measured. PlasmoDB GO terms were used for GO term mapping. Enrichment in molecular function GO terms was tested with the Fisher exact test using the weight-algorithm in topGO.[71] All terms with a p-value less than 0.05 were considered significant. GO terms represented by fewer than five proteins in the background dataset were excluded from the analysis.

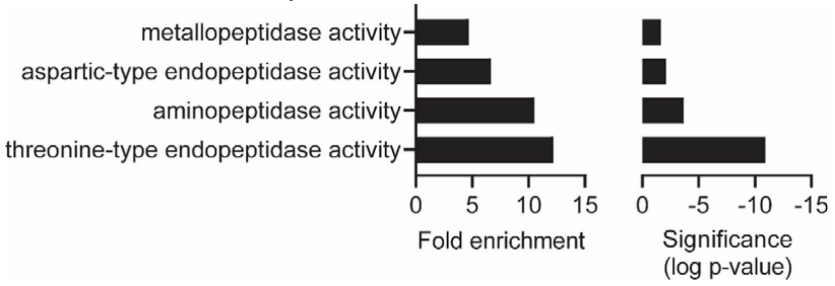

Supplemental Table S1. Related to Fig. 1

Percent inhibition by MIPS2673 of *Pf*A-M1 and *Pv*A-M1 aminopeptidase activities compared to selected human M1 homologues.

Concentration (μM)	% inhibition (%)[a]				
	*Pf*A-M1	*Pv*A-M1	LTA4H	ERAP1	ERAP2
1.25	100	100	0	0	31
10	100	100	58	2.3	0
500	-	-	42.2	89.8	97.8
1000	-	-	53.4	95.6	98.7

Supplemental Table S2. Related to Fig. 1

Cytotoxicity of MIPS2673 against the human HEK293 cell line.

Compound	% inhibition[a]	
	40 μM	120 μM
MIPS2673	NI	89
Puromycin[b]	100	103
Chloroquine	67	65
DHA	29	32

Supplemental Table S3. Related to Fig. 1

MIPS2673 effectiveness against a panel of drug resistant *P. falciparum* strains[a].

P. falciparum strain	Sensitivity profile	EC_{50} (nM)[b]	Fold shift in EC_{50} relative to	
			NF54	Dd2
NF54	Sensitive	237	1.0	
K1	Decreased sensitivity to chloroquine	278	1.2	
7G8	Decreased sensitivity to chloroquine	293	1.2	
TM90C2B	Decreased sensitivity to atovaquone	194	0.8	
Cam3.1	Decreased sensitivity to artemisinin	244	1.0	
Dd2	Decreased sensitivity to chloroquine	220	0.9	1.0
Dd2 DDD107498	Decreased sensitivity to eEF2 inhibitor, DDD107498	211		1.0
Dd2 MMV390048	Decreased sensitivity to PI4K inhibitor, MMV390048	164		0.7
Dd2 DSM265	Decreased sensitivity to DHODH inhibitor, DSM265	183		0.8
Dd2 GNF156	Decreased sensitivity to GNF156	195		0.9
Dd2 ELQ300	Decreased sensitivity to cyt bc1 inhibitor, ELQ300	174		0.8

Supplemental Table S4. Related to Fig. 1

MIPS2673 effectiveness against *P. falciparum* early (I-III)-, late (IV-V)-, and mature (V) gametocyte stages of NF54-pfs16-GFP parasites.

Compound	EC_{50} (nM)[a]		
	Early-stage Gametocytes	Late-stage Gametocytes	Mature-stage Gametocytes
MIPS2673	1660 ± 71	5300 ± 1923	98% (120 μM)[b]
Artesunate	16 ± 5.0	26 ± 2.0	51 ± 23

Supplemental Table S5. Related to Fig. 1

Data collection and refinement statistics.

	M1 MIPS2673
PDB ID	8SLO
Data collection statistics	
Wavelength	0.953700
Resolution range	41.4 - 1.55 (1.605 - 1.55)
Space group	P 21 21 21
Unit cell	76.4 108.5 117.6 90 90 90
Total reflections	1038039 (39097)
Unique reflections	139690 (12944)
Multiplicity	7.4 (6.4)
Completeness (%)	98.39 (91.92)
Mean I/sigma(I)	8.5 (0.9)
Wilson B-factor	17.19
R-pim (all I+ & I-)	0.057 (0.772)
CC1/2	0.997 (0.385)
Data Refinement statistics	
Reflections used in refinement	139628 (12905)
Reflections used for R-free	7039 (646)
R-work	0.1712 (0.2886)
R-free	0.2021 (0.3072)
Number of non-hydrogen atoms	8774
macromolecules	7432
ligands	45
solvent	1297
Protein residues	889
RMS(bonds)	0.007
RMS(angles)	0.88
Ramachandran favored (%)	98.20
Ramachandran allowed (%)	1.69
Ramachandran outliers (%)	0.11
Rotamer outliers (%)	0.24
Clashscore	2.35
Average B-factor	21.92
macromolecules	20.04
ligands	19.42
solvent	32.76

References

1 WHO (2022) **World Malaria Report 2022**

2 Price R.N., Commons R.J., Battle K.E., Thriemer K., Mendis K. (2020) **Plasmodium vivax in the Era of the Shrinking P. falciparum Map** *Trends Parasitol* **36**:560–570 https://doi.org/10.1016/j.pt.2020.03.009

3 Phillips M.A., Burrows J.N., Manyando C., van Huijsduijnen R.H., Van Voorhis W.C., Wells T.N.C. (2017) **Malaria** *Nat. Rev. Dis. Primers* **3** https://doi.org/10.1038/nrdp.2017.50

4 van der Pluijm R.W. *et al.* (2019) **Determinants of dihydroartemisinin-piperaquine treatment failure in Plasmodium falciparum malaria in Cambodia, Thailand, and Vietnam: a prospective clinical, pharmacological, and genetic study** *Lancet Infect. Dis* **19**:952–961 https://doi.org/10.1016/S1473-3099(19)30391-3

5 Balikagala B. *et al.* (2021) **Evidence of artemisinin-resistant malaria in Africa** *N. Engl. J. Med.* **385**:1163–1171 https://doi.org/10.1056/NEJMoa2101746

6 Liu J., Istvan E.S., Gluzman I.Y., Gross J., Goldberg D.E. (2006) **Plasmodium falciparum ensures its amino acid supply with multiple acquisition pathways and redundant proteolytic enzyme systems** *Proc. Natl. Acad. Sci. U. S. A.* **103**:8840–8845 https://doi.org/10.1073/pnas.0601876103

7 Lew V.L., Tiffert T., Ginsburg H. (2003) **Excess hemoglobin digestion and the osmotic stability of Plasmodium falciparum–infected red blood cells** *Blood* **101**:4189–4194 https://doi.org/10.1182/blood-2002-08-2654

8 Krugliak M., Zhang J., Ginsburg H. (2002) **Intraerythrocytic Plasmodium falciparum utilizes only a fraction of the amino acids derived from the digestion of host cell cytosol for the biosynthesis of its proteins** *Mol. Biochem. Parasitol.* **119**:249–256 https://doi.org/10.1016/S0166-6851(01)00427-3

9 Loria P., Miller S., Foley M., Tilley L. (1999) **Inhibition of the peroxidative degradation of haem as the basis of action of chloroquine and other quinoline antimalarials** *Biochem. J* **339**:363–370

10 Goldberg D.E. *et al.* (2005) **Hemoglobin degradation** *Malaria: Drugs, disease and post-genomic biology* :275–291 https://doi.org/10.1007/3-540-29088-5_11

11 Edgar R.C.S. *et al.* (2022) **Genetic and chemical validation of Plasmodium falciparum aminopeptidase PfA-M17 as a drug target in the hemoglobin digestion pathway** *eLife* **11** https://doi.org/10.7554/eLife.80813

12 Dalal S., Klemba M. (2007) **Roles for two aminopeptidases in vacuolar hemoglobin catabolism in Plasmodium falciparum** *J. Biol. Chem.* **282**:35978–35987 https://doi.org/10.1074/jbc.M703643200

13 Skinner-Adams T.S., Lowther J., Teuscher F., Stack C.M., Grembecka J., Mucha A., Kafarski P., Trenholme K.R., Dalton J.P., Gardiner D.L. (2007) **Identification of Phosphinate Dipeptide Analog Inhibitors Directed against the Plasmodium falciparum M17 Leucine Aminopeptidase as Lead Antimalarial Compounds** *J. Med. Chem.* **50**:6024–6031 https://doi.org/10.1021/jm070733v

14 Skinner-Adams T.S. *et al.* (2012) **The Aminopeptidase Inhibitor CHR-2863 Is an Orally Bioavailable Inhibitor of Murine Malaria** *Antimicrob. Agents Chemother.* **56**:3244–3249 https://doi.org/10.1128/AAC.06245-11

15 Harbut M.B., Velmourougane G., Dalal S., Reiss G., Whisstock J.C., Onder O., Brisson D., McGowan S., Klemba M., Greenbaum D.C. (2011) **Bestatin-based chemical biology strategy reveals distinct roles for malaria M1- and M17-family aminopeptidases** *Proc. Natl. Acad. Sci. U. S. A.* **108**:E526–534 https://doi.org/10.1073/pnas.1105601108

16 McGowan S. (2013) **Working in concert: the metalloaminopeptidases from Plasmodium falciparum** *Curr. Opin. Struct. Biol.* **23**:828–835 https://doi.org/10.1016/j.sbi.2013.07.015

17 Nankya-Kitaka M.F., Curley G.P., Gavigan C.S., Bell A., Dalton J.P. (1998) **Plasmodium chabaudi chabaudi and P. falciparum: inhibition of aminopeptidase and parasite growth by bestatin and nitrobestatin** *Parasitol. Res.* **84**:552–558 https://doi.org/10.1007/s004360050447

18 Bounaadja L., Schmitt M., Albrecht S., Mouray E., Tarnus C., Florent I. (2017) **Selective inhibition of PfA-M1, over PfA-M17, by an amino-benzosuberone derivative blocks malaria parasites development in vitro and in vivo** *Malar. J.* **16** https://doi.org/10.1186/s12936-017-2032-4

19 Deprez-Poulain R., Flipo M., Piveteau C., Leroux F., Dassonneville S., Florent I., Maes L., Cos P., Deprez B. (2012) **Structure–Activity Relationships and Blood Distribution of Antiplasmodial Aminopeptidase-1 Inhibitors** *J. Med. Chem.* **55**:10909–10917 https://doi.org/10.1021/jm301506h

20 Drinkwater N. *et al.* (2016) **Potent dual inhibitors of Plasmodium falciparum M1 and M17 aminopeptidases through optimization of S1 pocket interactions** *European Journal of Medicinal Chemistry* **110**:43–64 https://doi.org/10.1016/j.ejmech.2016.01.015

21 Vinh N.B. *et al.* (2019) **Hydroxamic Acid Inhibitors Provide Cross-Species Inhibition of Plasmodium M1 and M17 Aminopeptidases** *J. Med. Chem.* **62**:622–640 https://doi.org/10.1021/acs.jmedchem.8b01310

22 Gonzalez-Bacerio J., Fando R., Monte-Martinez d.A., Charli J.-L., Chávez d.l.A.M. (2014) **Plasmodium falciparum M1-Aminopeptidase: A Promising Target for the Development of Antimalarials** *Current Drug Targets* **15**:1144–1165 https://doi.org/10.2174/1389450115666141024115641

23 Mistry S.N. *et al.* (2014) **Two-Pronged Attack: Dual Inhibition of Plasmodium falciparum M1 and M17 Metalloaminopeptidases by a Novel Series of Hydroxamic Acid-Based Inhibitors** *J. Med. Chem.* **57**:9168–9183 https://doi.org/10.1021/jm501323a

24 Ruggeri C., Drinkwater N., Sivaraman K.K., Bamert R.S., McGowan S., Paiardini A. (2015) **Identification and Validation of a Potent Dual Inhibitor of the P. falciparum M1 and M17 Aminopeptidases Using Virtual Screening** *PLoS One* **10** https://doi.org/10.1371/journal.pone.0138957

25 Kannan Sivaraman K., Paiardini A., Sieńczyk M., Ruggeri C., Oellig C.A., Dalton J.P., Scammells P.J., Drag M., McGowan S. (2013) **Synthesis and Structure–Activity Relationships of Phosphonic Arginine Mimetics as Inhibitors of the M1 and M17 Aminopeptidases from Plasmodium falciparum** *J. Med. Chem.* **56**:5213–5217 https://doi.org/10.1021/jm4005972

26 Allary M., Schrevel J., Florent I. (2002) **Properties, stage-dependent expression and localization of Plasmodium falciparum M1 family zinc-aminopeptidase** *Parasitology* **125**:1–10 https://doi.org/10.1017/S0031182002001828

27 Azimzadeh O., Sow C., Gèze M., Nyalwidhe J., Florent I. (2010) **Plasmodium falciparum PfA-M1 aminopeptidase is trafficked via the parasitophorous vacuole and marginally delivered to the food vacuole** *Malar. J.* **9** https://doi.org/10.1186/1475-2875-9-189

28 Mathew R., Wunderlich J., Thivierge K., Cwiklinski K., Dumont C., Tilley L., Rohrbach P., Dalton J.P. (2021) **Biochemical and cellular characterisation of the Plasmodium falciparum M1 alanyl aminopeptidase (PfM1AAP) and M17 leucyl aminopeptidase (PfM17LAP)** *Sci. Rep.* **11** https://doi.org/10.1038/s41598-021-82499-4

29 Poreba M., McGowan S., Skinner-Adams T.S., Trenholme K.R., Gardiner D.L., Whisstock J.C., To J., Salvesen G.S., Dalton J.P., Drag M. (2012) **Fingerprinting the Substrate Specificity of M1 and M17 Aminopeptidases of Human Malaria, Plasmodium falciparum** *PLoS One* **7** https://doi.org/10.1371/journal.pone.0031938

30 McGowan S., Porter C.J., Lowther J., Stack C.M., Golding S.J., Skinner-Adams T.S., Trenholme K.R., Teuscher F., Donnelly S.M., Grembecka J. (2009) **Structural basis for the inhibition of the essential Plasmodium falciparum M1 neutral aminopeptidase** *Proceedings of the National Academy of Sciences* **106**:2537–2542 https://doi.org/10.1073/pnas.0807398106

31 Flipo M., Beghyn T., Leroux V., Florent I., Deprez B.P., Deprez-Poulain R.F. (2007) **Novel Selective Inhibitors of the Zinc Plasmodial Aminopeptidase PfA-M1 as Potential Antimalarial Agents** *J. Med. Chem.* **50**:1322–1334 https://doi.org/10.1021/jm061169b

32 Harbut M.B., Velmourougane G., Reiss G., Chandramohanadas R., Greenbaum D.C. (2008) **Development of bestatin-based activity-based probes for metallo-aminopeptidases** *Bioorg. Med. Chem. Lett.* **18**:5932–5936 https://doi.org/10.1016/j.bmcl.2008.09.021

33 Velmourougane G., Harbut M.B., Dalal S., McGowan S., Oellig C.A., Meinhardt N., Whisstock J.C., Klemba M., Greenbaum D.C. (2011) **Synthesis of New (–)-Bestatin-Based Inhibitor Libraries Reveals a Novel Binding Mode in the S1 Pocket of the Essential Malaria M1 Metalloaminopeptidase** *J. Med. Chem.* **54**:1655–1666 https://doi.org/10.1021/jm101227t

34 McGowan S. *et al.* (2010) **Structure of the Plasmodium falciparum M17 aminopeptidase and significance for the design of drugs targeting the neutral exopeptidases** *Proceedings of the National Academy of Sciences* **107**:2449–2454 https://doi.org/10.1073/pnas.0911813107

35 Challis M.P., Devine S.M., Creek D.J. (2022) **Current and emerging target identification methods for novel antimalarials** *Int. J. Parasitol. Drugs Drug Resist.* **20**:135–144 https://doi.org/10.1016/j.ijpddr.2022.11.001

36 Bailey B.L., Nguyen W., Cowman A.F., Sleebs B.E. (2023) **Chemo-proteomics in antimalarial target identification and engagement** *Med. Res. Rev* https://doi.org/10.1002/med.21975

37 Carolino K., Winzeler E.A. (2020) **The antimalarial resistome – finding new drug targets and their modes of action** *Current Opinion in Microbiology* **57**:49–55 https://doi.org/10.1016/j.mib.2020.06.004

38 Baragana B. *et al.* (2015) **A novel multiple-stage antimalarial agent that inhibits protein synthesis** *Nature* **522**:315–320 https://doi.org/10.1038/nature14451

39 Summers R.L. *et al.* (2021) **Chemogenomics identifies acetyl-coenzyme A synthetase as a target for malaria treatment and prevention** *Cell Chem. Biol* https://doi.org/10.1016/j.chembiol.2021.07.010

40 Cowell A.N. *et al.* (2018) **Mapping the malaria parasite druggable genome by using in vitro evolution and chemogenomics** *Science* **359**:191–199 https://doi.org/10.1126/science.aan4472

41 Flannery E.L. *et al.* (2015) **Mutations in the P-Type Cation-Transporter ATPase 4, PfATP4, Mediate Resistance to Both Aminopyrazole and Spiroindolone Antimalarials** *ACS Chem. Biol.* **10**:413–420 https://doi.org/10.1021/cb500616x

42 Yang T. *et al.* (2021) **MalDA, Accelerating Malaria Drug Discovery** *Trends Parasitol.* **37**:493–507 https://doi.org/10.1016/j.pt.2021.01.009

43 Siddiqui G. *et al.* (2022) **Peroxide antimalarial drugs target redox homeostasis in Plasmodium falciparum infected red blood cells** *ACS Infect. Dis.* https://doi.org/10.1021/acsinfecdis.1c00550

44 Molina D.M., Jafari R., Ignatushchenko M., Seki T., Larsson E.A., Dan C., Sreekumar L., Cao Y., Nordlund P. (2013) **Monitoring drug target engagement in cells and tissues using the cellular thermal shift assay** *Science* **341**:84–87 https://doi.org/10.1126/science.1233606

45 Dziekan J.M., Yu H., Chen D., Dai L., Wirjanata G., Larsson A., Prabhu N., Sobota R.M., Bozdech Z., Nordlund P. (2019) **Identifying purine nucleoside phosphorylase as the target of quinine using cellular thermal shift assay** *Sci. Transl. Med.* **11** https://doi.org/10.1126/scitranslmed.aau3174

46 Piazza I. *et al.* (2020) **A machine learning-based chemoproteomic approach to identify drug targets and binding sites in complex proteomes** *Nat. Commun.* **11** https://doi.org/10.1038/s41467-020-18071-x

47 Wirjanata G. *et al.* (2021) **Identification of an inhibitory pocket in falcilysin bound by chloroquine provides a new avenue for malaria drug development** *bioRxiv* https://doi.org/10.1101/2021.04.08.438947

48 Gavigan C.S., Dalton J.P., Bell A. (2001) **The role of aminopeptidases in haemoglobin degradation in Plasmodium falciparum-infected erythrocytes** *Molecular and biochemical parasitology* **117**:37–48 https://doi.org/10.1016/S0166-6851(01)00327-9

49 Yang T., Xie S.C., Cao P., Giannangelo C., McCaw J., Creek D.J., Charman S.A., Klonis N., Tilley L. (2016) **Comparison of the exposure time-dependence of the activities of synthetic ozonide antimalarials and dihydroartemisinin against K13 wild-type and mutant Plasmodium falciparum strains** *Antimicrob. Agents Chemother.* **60**:4501–4510 https://doi.org/10.1128/AAC.00574-16

50 Zhang M. *et al.* (2018) **Uncovering the essential genes of the human malaria parasite Plasmodium falciparum by saturation mutagenesis** *Science* **360** https://doi.org/10.1126/science.aap7847

51 Siddiqui G., De Paoli A., MacRaild C.A., Sexton A.E., Boulet C., Shah A.D., Batty M.B., Schittenhelm R.B., Carvalho T.G., Creek D.J. (2022) **A new mass spectral library for high-coverage and reproducible analysis of the Plasmodium falciparum–infected red blood cell proteome** *GigaScience* **11** https://doi.org/10.1093/gigascience/giac008

52 George A.L., Sidgwick F.R., Watt J.E., Martin M.P., Trost M., Marín-Rubio J.L., Dueñas M.E. (2023) **Comparison of Quantitative Mass Spectrometric Methods for Drug Target Identification by Thermal Proteome Profiling** *J Proteome Res.* https://doi.org/10.1021/acs.jproteome.3c00111

53 Dziekan J.M. *et al.* (2020) **Cellular thermal shift assay for the identification of drug–target interactions in the Plasmodium falciparum proteome** *Nat. Protoc.* **15**:1881–1921 https://doi.org/10.1038/s41596-020-0310-z

54 Piazza I., Kochanowski K., Cappelletti V., Fuhrer T., Noor E., Sauer U., Picotti P. (2018) **A Map of Protein-Metabolite Interactions Reveals Principles of Chemical Communication** *Cell* **172**:358–372 https://doi.org/10.1016/j.cell.2017.12.006

55 Creek D.J., Chua H.H., Cobbold S.A., Nijagal B., MacRae J.I., Dickerman B.K., Gilson P.R., Ralph S.A., McConville M.J. (2016) **Metabolomics-based screening of the malaria box reveals both novel and established mechanisms of action** *Antimicrob. Agents Chemother.* **60**:6650–6663 https://doi.org/10.1128/aac.01226-16

56 Giannangelo C., Siddiqui G., De Paoli A., Anderson B.M., Edgington-Mitchell L.E., Charman S.A., Creek D.J. (2020) **System-wide biochemical analysis reveals ozonide antimalarials initially act by disrupting Plasmodium falciparum haemoglobin digestion** *PLoS Pathog.* **16** https://doi.org/10.1371/journal.ppat.1008485

57 Birrell G.W., Challis M.P., De Paoli A., Anderson D., Devine S.M., Heffernan G.D., Jacobus D.P., Edstein M.D., Siddiqui G., Creek D.J. (2020) **Multi-omic characterization of the mode of action of a potent new antimalarial compound, JPC-3210, Against Plasmodium falciparum** *Mol. Cell. Proteomics* **19**:308–325 https://doi.org/10.1074/mcp.RA119.001797

58 Milne R. *et al.* (2022) **Toolkit of Approaches To Support Target-Focused Drug Discovery for Plasmodium falciparum Lysyl tRNA Synthetase** *ACS Infect. Dis.* **8**:1962–1974 https://doi.org/10.1021/acsinfecdis.2c00364

59 Gillet L.C., Navarro P., Tate S., Röst H., Selevsek N., Reiter L., Bonner R., Aebersold R. (2012) **Targeted Data Extraction of the MS/MS Spectra Generated by Data-independent Acquisition: A New Concept for Consistent and Accurate Proteome Analysis** *Mol. Cell. Proteomics* **11** https://doi.org/10.1074/mcp.O111.016717

60 Papakyriakou A., Stratikos E. (2017) **The role of conformational dynamics in antigen trimming by intracellular aminopeptidases** *Front. Immunol* **8** https://doi.org/10.3389/fimmu.2017.00946

61 Moore D.S., Brines C., Jewhurst H., Dalton J.P., Tikhonova I.G. (2018) **Steered molecular dynamics simulations reveal critical residues for (un)binding of substrates, inhibitors and a product to the malarial M1 aminopeptidase** *PLoS Comput. Biol.* **14** https://doi.org/10.1371/journal.pcbi.1006525

62 Shang X. *et al.* (2022) **Genome-wide landscape of ApiAP2 transcription factors reveals a heterochromatin-associated regulatory network during Plasmodium falciparum blood-stage development** *Nucleic Acids Res.* **50**:3413–3431 https://doi.org/10.1093/nar/gkac176

63 Ragheb D., Dalal S., Bompiani K.M., Ray W.K., Klemba M. (2011) **Distribution and biochemical properties of an M1-family aminopeptidase in Plasmodium falciparum indicate a role in vacuolar hemoglobin catabolism** *J. Biol. Chem.* **286**:27255–27265 https://doi.org/10.1074/jbc.M111.225318

64 Plouffe D. *et al.* (2008) **In silico activity profiling reveals the mechanism of action of antimalarials discovered in a high-throughput screen** *Proceedings of the National Academy of Sciences of the United States of America* **105**:9059–9064 https://doi.org/10.1073/pnas.0802982105

65 Gamo F.J. *et al.* (2010) **Thousands of chemical starting points for antimalarial lead identification** *Nature* **465**:305–310 https://doi.org/10.1038/nature09107

66 Guiguemde W.A., Shelat A.A., Garcia-Bustos J.F., Diagana T.T., Gamo F.J., Guy R.K. (2012) **Global phenotypic screening for antimalarials** *Chem Biol* **19**:116–129 https://doi.org/10.1016/j.chembiol.2012.01.004

67 Trager W., Jensen J.B. (1976) **Human malaria parasites in continuous culture** *Science* **193**:673–675 https://doi.org/10.1126/science.781840

68 Lambros C., Vanderberg J.P. (1979) **Synchronization of Plasmodium falciparum erythrocytic stages in culture** *J. Parasitol.* **65**:418–420 https://doi.org/10.2307/3280287

69 Rappsilber J., Ishihama Y., Mann M. (2003) **Stop and go extraction tips for matrix-assisted laser desorption/ionization, nanoelectrospray, and LC/MS sample pretreatment in proteomics** *Anal. Chem.* **75**:663–670 https://doi.org/10.1021/ac026117i

70 Alexa A., Rahnenführer J. (2020) **topGO: Enrichment Analysis for Gene Ontology, R package version 2.42.0**

71 Alexa A., Rahnenführer J., Lengauer T. (2006) **Improved scoring of functional groups from gene expression data by decorrelating GO graph structure** *Bioinformatics* **22**:1600–1607 https://doi.org/10.1093/bioinformatics/btl140

72 Malcolm T.R., Swiderska K.W., Hayes B.K., Webb C.T., Drag M., Drinkwater N., McGowan S. (2021) **Mapping the substrate specificity of the Plasmodium M1 and M17 aminopeptidases** *Biochem. J.* **478**:2697–2713 https://doi.org/10.1042/bcj20210172

73 Drinkwater N., Sivaraman K.K., Bamert R.S., Rut W., Mohamed K., Vinh N.B., Scammells P.J., Drag M., McGowan S. (2016) **Structure and substrate fingerprint of aminopeptidase P from Plasmodium falciparum** *Biochem. J.* **473**:3189–3204 https://doi.org/10.1042/bcj20160550

74 Sivaraman K.K. *et al.* (2012) **X-ray crystal structure and specificity of the Plasmodium falciparum malaria aminopeptidase PfM18AAP** *J. Mol. Biol.* **422**:495–507 https://doi.org/10.1016/j.jmb.2012.06.006

75 Cowieson N.P. *et al.* (2015) **MX1: a bending-magnet crystallography beamline serving both chemical and macromolecular crystallography communities at the Australian Synchrotron** *Journal of Synchrotron Radiation* **22**:187–190 https://doi.org/10.1107/S1600577514021717

76 Kabsch W. (2010) **XDS. Acta Crystallogr** *D Biol. Crystallogr.* **66**:125–132 https://doi.org/10.1107/s0907444909047337

77 Evans P.R., Murshudov G.N. (2013) **How good are my data and what is the resolution?** *Acta Crystallographica Section D* **69**:1204–1214 https://doi.org/10.1107/S0907444913000061

78 Winn M.D. *et al.* (2011) **Overview of the CCP4 suite and current developments** *Acta Crystallogr. D Biol. Crystallogr.* **67**:235–242 https://doi.org/10.1107/s0907444910045749

79 McCoy A.J., Grosse-Kunstleve R.W., Adams P.D., Winn M.D., Storoni L.C., Read R.J. (2007) **Phaser crystallographic software** *J Appl Crystallogr* **40**:658–674 https://doi.org/10.1107/s0021889807021206

80 Adams P.D. *et al.* (2010) **PHENIX: a comprehensive Python-based system for macromolecular structure solution** *Acta Crystallogr. D Biol. Crystallogr.* **66**:213–221 https://doi.org/10.1107/s0907444909052925

81 Emsley P., Cowtan K. (2004) **Coot: model-building tools for molecular graphics** *Acta Crystallogr. D Biol. Crystallogr.* **60**:2126–2132 https://doi.org/10.1107/s0907444904019158

82 Emsley P., Lohkamp B., Scott W.G., Cowtan K. (2010) **Features and development of Coot** *Acta Crystallogr. D Biol. Crystallogr.* **66**:486–501 https://doi.org/10.1107/s0907444910007493

83 Smilkstein M., Sriwilaijaroen N., Kelly J.X., Wilairat P., Riscoe M. (2004) **Simple and inexpensive fluorescence-based technique for high-throughput antimalarial drug screening** *Antimicrob. Agents Chemother.* **48**:1803–1806 https://doi.org/10.1128/AAC.48.5.1803-1806.2004

84 Snyder C., Chollet J., Santo-Tomas J., Scheurer C., Wittlin S. (2007) **In vitro and in vivo interaction of synthetic peroxide RBx11160 (OZ277) with piperaquine in Plasmodium models** *Exp. Parasitol.* **115**:296–300 https://doi.org/10.1016/j.exppara.2006.09.016

85 Duffy S., Avery V.M. (2013) **Identification of inhibitors of Plasmodium falciparum gametocyte development** *Malar. J.* **12** https://doi.org/10.1186/1475-2875-12-408

86 Duffy S., Loganathan S., Holleran J.P., Avery V.M. (2016) **Large-scale production of Plasmodium falciparum gametocytes for malaria drug discovery** *Nat. Protoc.* **11**:976–992 https://doi.org/10.1038/nprot.2016.056

87 Lucantoni L., Loganathan S., Avery V.M. (2017) **The need to compare: assessing the level of agreement of three high-throughput assays against Plasmodium falciparum mature gametocytes** *Sci. Rep.* **7** https://doi.org/10.1038/srep45992

88 Duffy S., Avery V.M. (2012) **Development and Optimization of a Novel 384-Well Anti-Malarial Imaging Assay Validated for High-Throughput Screening** *The American Society of Tropical Medicine and Hygiene* **86**:84–92 https://doi.org/10.4269/ajtmh.2012.11-0302

89 Bevan C.D., Lloyd R.S. (2000) **A high-throughput screening method for the determination of aqueous drug solubility using laser nephelometry in microtiter plates** *Anal. Chem.* **72**:1781–1787 https://doi.org/10.1021/ac9912247

90 Perez-Riverol Y. *et al.* (2021) **The PRIDE database resources in 2022: a hub for mass spectrometry-based proteomics evidences** *Nucleic Acids Res* **50**:D543–D552 https://doi.org/10.1093/nar/gkab1038

Editors

Reviewing Editor
Dominique Soldati-Favre
University of Geneva, Geneva, Switzerland

Senior Editor
Dominique Soldati-Favre
University of Geneva, Geneva, Switzerland

Reviewer #1 (Public Review):

By using a series of biochemical methods based on proteomic and metabolomic approaches, this study aims at: (1) validating the specific targeting of a biologically active molecule (MIPS2673) towards a defined (and unique?) protein target within a parasite, and (2) exploring whether it is possible to extrapolate which metabolic pathway has been disrupted.

Strength/Weaknesses

-The chemoproteomic approach, convincingly shows that MIPS2673 more significantly "protects" the putative target (PfA-M1) against thermal degradation or against enzymatic attack (by proteinase K). Proteomic studies are carried using parasite extracts enriched in late trophozoites (30-38 h pi), and are restricted to the soluble proteins fraction.
-The metabolomic approach, documents the ability of MIPS2673 to selectively increase the number of non-hydrolyzed dipeptides in treated versus untreated parasites, further arguing for selective targeting of PfA-M1 and impairment of hemoglobin breakdown by the parasite.
-The revised version now also considers and further studies the additional putative targets identified by one proteomic approach (but not the other one), which is both more critical of the results obtained and more realistic.
The work as a whole is highly interesting, both for the specific topic of PfA-M1's role in parasite biology and for the method, applicable to other malarial drug contexts.

https://doi.org/10.7554/eLife.92990.2.sa2

Reviewer #2 (Public Review):

In this manuscript, the authors first developed a new small molecular inhibitor that could target specifically the M1 metalloproteases of both important malaria parasite species Plasmodium falciparum and P. vivax. This was done by a chemical modification of a previously developed molecule that targets PfM1 as well as PfM17 and possibly other Plasmodial metalloproteases. After the successful chemical synthesis, the authors showed that the derived inhibitor, named MIPS2673, has a strong antiparasitic activity with IC50 342 nM and it is highly specific for M1. With this in mind, the authors first carried out two large-scale proteomics to confirm the MIPS2673 interaction with PfM1 in the context of the total P. falciparum protein lysate. This was done first by using thermal shift profiling and subsequently limited proteolysis. While the first demonstrated overall interaction, the latter (limited proteolysis) could map more specifically the site of MIPS2673-PfM1 interaction, presumably the active site. Subsequent metabolomics analysis showed that MIPS2673 cytotoxic inhibitory effect leads to the accumulation of short peptides many of which originate from hemoglobin. Based on that the authors argue that the MIPS2673 mode of action (MOA) involves inhibition of hemoglobin digestion that in turn inhibits the parasite growth and development.

Comments on the revised version:

The authors addressed all my comments from the previous round of reviews.

https://doi.org/10.7554/eLife.92990.2.sa1

Reviewer #3 (Public Review):

Summary:

Overall, this is an interesting series of experiments which have identified a putative inhibitor of the Plasmodium M1 alanyl aminopeptidases, PfA-M1 and PvA-M1. The weaknesses include the lack of additional analysis of additional targets identified in the chemoproteomic approaches.

Strengths:

The main strengths include the synthesis of MIPS2673 which is selectively active against the enzyme and in whole cell assay.

Weaknesses:

The authors have addressed the previously identified weaknesses and have now provided additional data and explanations. They have modified their conclusions to indicate the limitations of their work.

https://doi.org/10.7554/eLife.92990.2.sa0

Author response:

The following is the authors' response to the original reviews.

> ***eLife assessment***
>
> *The manuscript constitutes an important contribution to antimalarial drug discovery, employing diverse systems biology methodologies; with a focus on an improved M1 metalloprotease inhibitor, the study provides convincing evidence of the utility of chemoproteomics in elucidating the preferential targeting of PfA-M1. Additionally, metabolomic analysis effectively documents specific alterations in the final steps of hemoglobin breakdown. These findings underscore the potential of the developed methodology, not only in understanding PfA-M1 targeting but also in its broader applicability to diverse malarial proteins or pathways. Revisions are needed to further enhance overall clarity and detail the scope of these implications.*

We thank the editor and reviewers for recognising the contribution our work makes to understanding the selective targeting of aminopeptidase inhibitors in malaria parasites and the wider impact this multi-omic strategy can have for anti-parasitic drug discovery efforts. The reviewers have provided constructive feedback and raised important points that we have taken on-board to improve our manuscript. In particular, we have revised aspects of the text and figures to enhance clarity, performed additional analysis on the other possible MIPS2673 interacting proteins and more comprehensively analysed the effect of MIPS2673 on parasite morphology. NB: Specific responses to comments in the public reviews are provided within responses to the specific recommendations to authors.

Public Reviews:

Reviewer #1 (Public Review):

Summary:

The article "Chemoproteomics validates selective targeting of Plasmodium M1 alanyl aminopeptidase as a cross-species strategy to treat malaria" presents a series of biochemical methods based on proteomics and metabolomics, as a means to:

(1) validate the specific targeting of biologically active molecules (MIPS2673) towards a defined (unique) protein target within a parasite and (2) to explore whether by quantifying the perturbations generated at the level of the parasite metabolome, it is possible to extrapolate which metabolic pathway has been disrupted by using this biologically active molecule and whether this may further confirm selective targeting in parasites of the expected (or in-vitro targeted) enzyme (here PfA-1).

The inhibitor used in this work by the authors (MIPS2673) is to my knowledge a novel one, although belonging to a chemical series previously explored by the authors, which recently enabled them to discover a specific PfA-M17 inhibitor, MIPS2571 (Edgard et al., 2022, ref 11 of this current work). Indeed, inhibitors specifically targeting either PfA-M1 or PfA-M17 (and not both, as currently done in the past) are scarce today, and highly needed to functionally characterize these two zinc-aminopeptidases. MIPS2673, blocks the development of erythrocytic stages of Plasmodium falciparum with an EC50 of 324 nM, blocks the parasite development at the young trophozoite stage at 5x EC50 (but at ring stages at 10xEC50, figure 1E), and inhibits the enzymatic activity of PfA-M1 (and its ortholog Pv-M1) but not of the related malarial metallo-aminopeptidases (M17 and M18 families) nor the human metalloenzymes from closely related enzymatic families, supporting its selective targeting of PfA-M1 (and Pv-M1).

All experiments are carried out in vitro (e.g. biochemical studies such as enzymology, proteomics, metabolomics) and on cultured parasites (erythrocyte stages of Plasmodium falciparum and several gametocytes stages obtained in vitro); there are no in vivo manipulations. The work related to Plasmodium vivax, which justifies the "cross-species" indication in the title of the article, is restricted to using a recombinant form of the M1-family aminopeptidase in enzymatic assays. The rest of the work concerns only Plasmodium falciparum. While I found globally that this work is original and brings new data and above all proposes chemical validation approaches that could be used for other target validations under similar limiting conditions (impossibility of KO of the gene), I have some specific questions to address to the authors.

Strengths and weaknesses:

- The chemoproteomic approach, that explores the ability of MIPS2673 to more significantly "protect" the putative target (PfA-M1) against thermal degradation or enzymatic attack (by proteinase K), to document its selective targeting towards PfA-M1 (the inhibitor, once associated with its target, is expected to stabilize its structure or prevent the action of end proteases), uses several concentrations of MIPS2673 and provides convincing results. My main criticism is that these tests are carried out with parasite extracts enriched in 30-38 hours old forms, and restricted to the fraction of soluble proteins isolated from these parasitic forms, which still limits the scope of the analysis. It is clear that this methodological approach is a choice that can be argued both biologically (PfA-M1 is well expressed in these stages of the parasite development) and biochemically (it is difficult to do proteomic analyses on insoluble proteins) but I regret that the authors do not discuss these limitations further, notably, I would have expected (from Figure 1E) some targets to be also present at ring stages.

- The metabolomic approach, by documenting the ability of MIPS2673 to selectively increase the number of non-hydrolyzed dipeptides in treated versus untreated parasites is another argument in favor of the selective targeting of PfA-M1 by MIPS2673, in particular by its broad-spectrum aminopeptidase action preferentially targeting peptides resulting from the degradation of hemoglobin by the parasite. The relative contribution of peptides derived from host hemoglobin versus other parasite proteins is, however, little discussed.

The work as a whole remains highly interesting, both for the specific topic of PfA-M1's role in parasite biology and for the method, applicable to other malarial drug contexts.

Reviewer #2 (Public Review):

In this manuscript, the authors first developed a new small molecular inhibitor that could target specifically the M1 metalloproteases of both important malaria parasite species Plasmodium falciparum and P. vivax. This was done by a chemical modification of a previously developed molecule that targets PfM1 as well as PfM17 and possibly other Plasmodial metalloproteases. After the successful chemical synthesis, the authors showed that the derived inhibitor, named MIPS2673, has a strong antiparasitic activity with IC50 342 nM and it is highly specific for M1. With this in mind, the authors first carried out two large-scale proteomics to confirm the MIPS2673 interaction with PfM1 in the context of the total P. falciparum protein lysate. This was done first by using thermal shift profiling and subsequently limited proteolysis. While the first demonstrated overall interaction, the latter (limited proteolysis) could map more specifically the site of MIPS2673-PfM1 interaction, presumably the active site. Subsequent metabolomics analysis showed that MIPS2673 cytotoxic inhibitory effect leads to the accumulation of short peptides many of which originate from hemoglobin. Based on that the authors argue that the MIPS2673 mode of action (MOA) involves inhibition of hemoglobin digestion that in turn inhibits the parasite growth and development.

Reviewer #3 (Public Review):

This is a manuscript that attempts to validate Plasmodium M1 alanyl aminopeptidase as a target for antimalarial drug development. The authors provide evidence that MIPS2673 inhibits recombinant enzymes from both Pf and Pv and is selective over other proteases. There is in vitro antimalarial activity. Chemoproteomic experiments demonstrate selective targeting of the PfA-M1 protease.

This is a continuation of previous work focused on designing inhibitors for aminopeptidases by a subset of these authors. Medicinal chemistry explorations resulted in the synthesis of MIPS2673 which has improved properties including potent inhibition of PfA-M1 and PvA-M1 with selectivity over a closed related peptidase. The compound also demonstrated selectivity over several human aminopeptidases and was not toxic to HEK293 cells at 40 uM. The activity against P. falciparum blood-stage parasites was about 300 nM.

Thermal stability studies confirmed that PfA-M1 was a binding target, however, there were other proteins consistently identified in the thermal stability studies. This raises the question as to their potential role as additional targets of this inhibitor. The authors dismiss these because they are not metalloproteases, but further analysis is warranted. This is particularly important as the authors were not able to generate mutants using in vitro evolution of resistance strategies. This often indicates that the inhibitor has more than one target.

The next set of experiments focused on a limited proteolysis approach. Again several proteins were identified as interacting with MIPS2673 including metalloproteases. The

authors go on to analyze the LiP-MS data to identify the peptide from PfA-M1 which putatively interacts with MIPS2673. The authors are clearly focused on PfA-M1 as the target, but a further analysis of the other proteins identified by this method would be warranted and would provide evidence to either support or refute the authors' conclusions.

The final set of experiments was an untargeted metabolomics analysis. They identified 97 peptides as significantly dysregulated after MIPS2673 treatment of infected cells and most of these peptides were derived from one of the hemoglobin chains. The accumulation of peptides was consistent with a block in hemoglobin digestion. This experiment does reveal a potential functional confirmation, but questions remain as to specificity.

Overall, this is an interesting series of experiments that have identified a putative inhibitor of PfA-M1 and PvA-M1. The work would be significantly strengthened by structure-aided analysis. It is unclear why putative binding sites cannot be analyzed via specific mutagenesis of the recombinant enzyme.

In the thermal stability and LiP -MS analysis, other proteins were consistently identified in addition to PfA-M1 and yet no additional analysis was undertaken to explore these as potential targets.

The metabolomics experiments were potentially interesting, but without significant additional work including different lengths of treatment and different stages of the parasite, the conclusions drawn are overstated. Many treatments disrupt hemoglobin digestion - either directly or indirectly and from the data presented here it is premature to conclude that treatment with MIPS2673 directly inhibits hemoglobin digestion.

Finally, the potency of this compound on parasites grown in vitro is 300 nM - this would need improvements in potency and demonstration of in vivo efficacy in the SCID mouse model to consider this a candidate for a drug.

Summary:

Overall, this is an interesting series of experiments that have identified a putative inhibitor of the Plasmodium M1 alanyl aminopeptidases, PfA-M1 and PvA-M1.

Strengths:

The main strengths include the synthesis of MIPS2673 which is selectively active against the enzymes and in whole-cell assay.

Weaknesses:

The weaknesses include the lack of additional analysis of additional targets identified in the chemoproteomic approaches.

Recommendations for the authors:

Reviewer #1 (Recommendations For The Authors):

Question 1. Line 737 (and elsewhere). Why are Plasmodium vivax orthologs of PfA-M1 and PfA-M17 called Pv-M1 and Pv-M17 and not PvA-M1 and PvA-M17, where A stands for Aminopeptidase? I would recommend changing the names if possible, although the mention of Pv-M1 and Pv-M17 is now current in the literature (which is kind of regrettable). See also Supplemental Table S1 where PfA-M1 is named Pf-M1.

Supplemental Table S1 was updated to PfA-M1. Nomenclature for the Plasmodium vivax aminopeptidase orthologs was amended to PvA-M1 and PvA-M17 as suggested by the reviewer.

> *Question 2. Figure 1. Observation of parasite culture slide smears in Figure 1E strongly suggests that an important target of MIPS2673 appears to be expressed at the ring stage or very young trophozoites, whereas the authors, in their proteomic and metabolomic analyses, performed studies focused on late trophozoites stages (30-38h post-invasion). This difference in the targeting of Plasmodium stages puzzles me and deserves some explanations from the authors, and is related to my question 3.*

As the reviewer indicates, ring-stage parasite growth appears to be affected at high concentrations (5x and 10x EC50) of MIPS2673. Under these conditions, parasite growth appears to stall during late rings/early trophs at ~16-22 h post invasion when haemoglobin digestion is increasing and when one presumes PfA-M1 (the primary target of MIPS2673) is increasing in both expression and activity (see references 26 and 28 of this manuscript). Thus, whilst it is unsurprising that MIPS2673 has some activity against ring-stage parasites, we focused on the trophozoite stage for our proteomics studies as we showed this to be the stage most susceptible to MIPS2673 (Fig. 1D) and reasoned that we would most likely identify the primary MIPS2673 target, and other interacting proteins, from a complex biological mixture at this stage. The same reasoning underpinned our decision to perform metabolomics on drug-treated trophozoites, as we reasoned we would see a greater functional effect on this stage. Furthermore, performing these experiments on trophozoites rather than rings minimises the interference from the host red blood cell. While we cannot rule out additional targets in rings, repeating all experiments during this parasite stage is beyond the scope of this study.

> *Question 3. Figure 2. Although Figure 2 is insightful and somehow self-explanatory, I think it misses two specific pieces of information. First, it is indicated in line 618 (M&M) that parasite material for thermal stability and limited proteolysis studies correspond to synchronized parasites (30-38h post-invasion) but this information is not given in Figure 2. In addition, if I fully understand the experimental protocol of obtaining parasite extracts, they strictly correspond to the soluble protein fraction of the erythrocytic stages of plasmodium at the late trophozoite stage, and not to all parasitic proteins as the scheme of Figure 2 might suggest. I would appreciate it very much if these two points (parasite stages and soluble proteins) were clearly indicated in the scheme as indeed, not the whole parasite blood stage proteome is investigated in the study but just a part of it (~47%, as the authors indeed indicate line 406). Please, edit also the legend of the figure accordingly.*

This is correct, the soluble protein fraction from synchronised trophozoites was used in our proteomics studies. These details have been included in an updated Figure 2 and in the corresponding figure legend.

> *Question 4. Thermal stabilization. Figure 3B. Could the authors explain how they calculated or measured "absolute" protein abundances, and how this refers to a number of parasites in initial assays as this is not clear to me. Notably, abundance for PfA-M1 is much higher than for PF3D7_0604300, which are interesting "absolute" values.*

Protein abundance was calculated using the mean peptide quantity of the stripped peptide sequence, with only precursors passing the Q-value threshold (0.01) considered for relative quantification. Within independent experiments, normalisation was based on total protein amount (determined by the BCA assay) rather than the initial number of parasites.

PfA-M1 is known to be a highly abundant protein and PF3D7_0604300 (as well as the other protein hits identified by thermal stability proteomics) are likely less abundant. It is noted that abundance is also dependent on ionisation efficiency and trypsin digestion efficiency. Therefore, we avoid comparing absolute abundances across proteins and use relative differences across conditions instead.

NB: the word “absolute” in the text (“absolute fold-change”) refers to the absolute value of the fold-change (i.e. positive or negative), and not to absolute quantification of proteins. The preceding text in each case clarifies that these are based on “relative peptide abundance”.

> *Question 5. Figure 5A. How do the authors explain peptides whose abundances are decreasing instead of increasing? Figure 5C. Could the authors provide digital cues (aa numbers or positions) on the ribbon representation of the PfA-M1 sequence? It is difficult to correlate the position of the 3D domains with respect to the primary structure of the protein. Also, the "yellow" supposed to show the "drug ligand" is really not very visible.*

LiP-MS is based on the principle that ligand binding alters the local proteolytic susceptibility of a protein to a non-specific protease (in this case proteinase K, PK). In this sense, in LiP-MS we are not looking at variations in the stability of whole proteins (as is the case with thermal stability proteomics, where proteins detected with significantly higher abundance in treated relative to control samples reflects thermal stabilisation of the target due to ligand binding), but differences in peptide patterns between treated and control samples that reflect a change in the ability of PK to cleave the target. Thus, in the bound state, the ligand prevents proteolysis with PK. This results in decreased abundance of peptides with non-tryptic ends (as PK cannot access the region around where the ligand is bound) and increased abundance of the corresponding fully tryptic peptide, when compared to the free target. This concept is demonstrated in Fig. 4A and is explained in the text (lines 279-282) and Fig. 4 figure legend.

To aid visualisation, we have not added amino acid positions on the PfA-M1 sequence in Fig. 5, but have provided amino acid positions for all peptides in Supplementary File 3. We have also changed the colour of the ligand in Fig. 5C to blue and increased transparency of the binding and centre of mass neighbourhoods.

> *Question 6. Gametocyte assays. Line 824 states that several compounds were used as positive controls for anti-gametocyte activity (chloroquine, artesunate, pyronaridine, pyrimethamine, dihydroartemisinin, and methylene blue) and line 821 states that the biological effects are measured against puromycin. This is not very clear to me, could the authors comment on this?*

This wording has been clarified in the methods to reflect that 5 µM puromycin was used as the positive control to calculate percent viability, whereas the other antimalarials were run in parallel as reference compounds with known anti-gametocyte activity (line 862).

> *Question 7. Metabolomics. Metabolomic assays were done on parasites at 28h pi, incubated for 1h with 3x EC50 of MIPS2673. You mention applying the drug on 2x10E8 infected red blood cells (line 838) but you do not explain how you isolate these infected red blood cells from non-infected red blood cells. Could you please specify this?*

Metabolomics studies were performed such that cultures at 2% haematocrit and 6% trophozoite-stage parasitaemia (representing 2 x 108 cells in total, rather than 2 x 108 infected cells) were treated with compound or vehicle and after 1 h metabolites were extracted. This methodological detail has been clarified in the methods (line 875).

> *Question 8. Figure 3B. Does this diagram come from the experimental 3D structure created by the authors (8SLO) or from molecular modeling? Please specify in the legend (line 1305).*

The diagram showing the binding mode of MIPS2673 bound to PfA-M1 comes from the experimentally determined 3D structure (PDB ID: 8SLO). This has now been stated in the figure legend. Note that the structural diagram refers to Fig. 1B (not Fig. 3B as indicated by the reviewer). The experimentally determined PfA-M1 structure with MIPS2673 bound (PDB ID: 8SLO) was also used to map LiP peptides and estimate the MIPS2673 binding site in Fig. 5, which is also now reflected in the appropriate section of the text (line 308) and Fig. 5 legend.

> *Question 9. Line 745. Why not indicate µm concentration for this H-Leu-NHMec substrate while it is indicated for the other substrates mentioned in the rest of the paragraph (H-Ala-NHMec, 20 µM, etc..). Also in this section (Enzyme assays) the pH at which the various enzymatic assays were done is missing.*

All enzyme assays were performed at pH 8.0. The concentration of H-Leu-NHMec varied depending on the enzyme assayed, as follows: 20 µM for PfA-M1, 40 µM for PvA-M1 and 100 µM for ERAP1 and ERAP2. This information is now clearly stated in the methods section (lines 782 and 787) and as a footnote for Supplemental Table S1.

> *Question 10. Line 830, please define FBS.*

Fetal bovine serum (FBS) has been added where appropriate (line 867).

> *Question 11. The authors mention in the title the targeting of several plasmodium species, but the only experimental study on the Plasmodium vivax species concerns the use of the recombinant enzyme Pv-M1. Authors also mention "multi-stage targets", but ultimately only look at erythrocyte stages and three different gametocyte stages.*

We have now removed the words “cross-species” and “multi-stage” from the manuscript title and abstract so as not to overstate these findings. We have also added the word “potential” in the manuscript text to clarify that selective M1 inhibition could offer a potential multistage and cross species strategy for malaria.

> *Question 12. Supplemental Table S1. I would suggest replacing "Percent inhibition by MIPS2673 of PfA-M1 and Pv-M1 aminopeptidases compared to selected human M1 homologues" with "Percent inhibition by MIPS2673 of PfA-M1 and Pv-M1 aminopeptidase activities compared to selected human M1 homologues".*

Done.

> *Question 13. Supplemental Table S3. Here you indicate IC50 while in text and Figure 1 you quote EC50. Why this difference?*

This has now been changed to EC50 in Supplemental Table S3.

> ***Reviewer #2 (Recommendations For The Authors):***
>
> *Amendments that I would recommend in order to improve the presentation include all four parts of the study:*
>
> *(1) In vitro antiparasitic activity of MIPS2673.*

> *The authors showed that MIPS2673 inhibits parasite growth with IC50 of 324nM measured by a standard drug sensitivity assay, Fig 1C. This is all well and good, but it would be helpful to include at least one if not more other compounds such as antimalaria drugs and/or their earlier inhibitors (e.g. inhibitor 1) for comparisons. This is typically done to show that the assay in this manuscript is fully compatible with previous studies. It will also give a better view of how the selective inhibition of PfM1 kills the parasite, specifically.*

Alongside MIPS2673, we also analysed the potency of the known antimalarial artesunate, which was found to have an EC50 of 4 nM. This value agrees with the expected potency of artesunate and indicates our MIPS2673 value of 324 nM is indeed compatible with previous studies. We have now reported the artesunate EC50 value for reference (lines 197-198 and Fig. S1).

> *Next, the authors proceeded to investigate the stage-specific effect of MIPS2673 but this time doing a survival assay instead of proper IC50 estimations (Figure 1. I wonder why? Drug survival assays have typically very limited information content and measuring proper IC50 in stage-specific wash-off assays would be much more informative.*

We performed single concentration stage specificity assays to determine the parasite asexual stage at which MIPS2673 is most active. This involved washing off the compound after a 24 h exposure in rings or trophozoites and determining parasite viability in the next asexual lifecycle. While a full dose response curve would allow generation of an EC50 value against the respective parasite stages, this information is unlikely to change the interpretation that MIPS2673 is more active against trophozoites stages than against rings.

> *Finally, in Figure 1E, the authors present the fact that the MIPS2673 arrests the parasite development. This is done by presenting a single (presumably representative) cell per time point. This is in my view highly insufficient. I recommend this figure be supplemented by parasite stage counts or other more comprehensive data representation. Also, the authors mention that while there is a growth arrest, hemoglobin is still being made. From the cell images, I can not see anything that supports this statement.*

We thank the reviewer for this constructive comment and they are correct in their assessment that these are representative parasite images at the respective time points. To address the reviewers concerns we have now provided cell counts from each treatment condition (Fig. 1E) at selected time points, which shows parasite stalling at the ring to trophozoite transition under drug treatment. On reflection, we agree that it is difficult to determine the presence of haemozoin from our images and have removed this statement.

> *(2) Protein thermal shift profiling. In the next step, the authors proceed to carry out cellular thermal shift profiling to show that PfM1 indeed interacts with MIPS2673, this time in the context of the total protein lysates from P. falciparum. This section of the study is in my view quite solid and indeed it is nice to see that the inhibitor causes a thermal shift of PfM1 which further supports what was already expected: interaction.*
>
> *I have no problem with this study in terms of the technical outcome but I would urge the authors to tone down the interpretation of these results in two ways.*
>
> *Four other proteins were found to be shifted by the inhibitor which also indicates interactions. Calling it simply "off-target" interactions might not represent the truth. The authors should explore and in some way comment that interactions with these proteins could contribute to the MIPS2673 MOA. I do not suggest conducting any more studies*

> *but simply acknowledge this situation. Identifying more than one target is indeed very common in CETSA studies and it would be helpful to acknowledge this here as well.*

We agree that identifying binding proteins in addition to the "expected" target is commonplace, and is indeed one of the benefits of this unbiased and proteome-wide approach. In the results and discussion, we have now amended our language to refer to these additional hits as MIPS2673-interacting proteins. In our original manuscript we dedicate a paragraph in the discussion to these additional interacting proteins and the likelihood of them being targets that contribute to antimalarial activity. Of these four additional interacting proteins, only the putative AP2 domain transcription factor (PF3D7_1239200) is predicted to be essential for blood stage growth and is therefore the only protein from this additional four that would likely contribute to antimalarial activity. These points are explicitly stated in the discussion (lines 530-550). Notably, all of the other interacting proteins identified in our thermal stability dataset were detected in our LiP-MS experiment but were not identified as interacting proteins by this method. The remaining three proteins were two non-essential *P. falciparum* proteins with unknown functions (PF3D7_1026000 and PF3D7_0604300) that are poorly described in the literature and a human protein (RAB39A). Further analysis of these other thermal stability proteomics hits in our LiP-MS dataset (see responses to Reviewer #3) identified none or only 1 significant LiP peptide from these proteins across our LiP-MS datasets, indicating they are likely to be false positive hits. Caveats around identifying protein targets by different deconvolution methods are also now addressed (lines 545-550).

> *At some point, the author argues that causing shifts of only four/five proteins including PfM1 shows that MIPS2673 does not interact with other (off) targets. Here one must be careful to present the lack of shifts in the CETSA as proof of no interaction. There are many reasons why thermal shifts are not observed including the physical properties of the individual proteins, detection limit etc. Again I suggest adjusting these statements accordingly.*

We thank the reviewer for raising this important point and have now included additional discussion around this comment (lines 545-550).

> *Finally, I am not convinced that Figure 2 presents nothing more than the overall experimental scheme with not much new information. Many of such schemes were published previously in the original publication of thermal profiling. I would suggest omitting it from the main text and shifting it into supplementary methods etc.*

We agree that similar schemes have been published previously, especially for thermal proteome profiling, and acknowledge the reviewer's suggestion of moving this figure to the supplemental material. However, we have kept Fig. 2 in the main text as this scheme also incorporates a LiP-MS workflow for malaria drug target deconvolution (the first to do so) and also to satisfy the additional details requested for this figure by Reviewer #1 (question 3).

> *(3) Identification of MIPS2673 target proteins using LiP-MS. In the next step, the authors carried out the limited proteolysis analysis with the rationale that protein peptides that are near the inhibitor binding site will exhibit higher resilience to proteolysis. The authors did a very good job of showing this for PfM1-MISP2673 interaction. This part is very impressive from a technological perspective, and I congratulate the authors on such achievement. I imagine these types of studies require very precise optimizations and performance.*
>
> *Here, however, I struggle with the meaning of this experiment for the overall flow of the manuscript. It seems that the binding pocket of MIPS2673 is less known since the*

> *inhibitor was designed for it. In fact, the authors mentioned that the crystal structure of PfM1 is available. From this perspective, the LiP-MS study represents more of a technical proof of concept for future drug target analysis but has limited contribution to the already quite well-established PfM1-MISP2673 interaction. Perhaps this could be presented in this way in the text.*

We thank the reviewer for this comment and they are correct that we solved the crystal structure of PfA-M1 bound to MIPS2673. We wish to highlight that the primary reason for performing the LiP-MS study was as an independent and complementary target deconvolution method to narrow down the shortlist of targets identified with thermal stability proteomics, and validate with high confidence that PfA-M1 is indeed the primary target of MIPS2673 in parasites. The use of a complementary approach based on a different biophysical principle (proteolytic susceptibility vs thermal stability) would also allow us to identify MIPS2673 interacting proteins that may not be detectable by thermal stability proteomics, for example targets that do not alter their thermal stability upon ligand binding. The text in the results and discussion has been amended to clarify these points (lines 266-268 and 545-550).

Furthermore, we agree that correctly predicting the MIPS2673 binding site on PfA-M1 using our LiP-MS peptide data is a technical proof of concept. Indeed, we wished to highlight the potential utility of LiP-MS for identifying both the protein targets of drugs and predicting their binding site, which is not possible with many other target deconvolution approaches. This point has been updated in the text (lines 303-304, 459-461).

> *(4) Metabolomic profiling of MIPS2673 inhibition showed a massive accumulation of short peptides which clearly indicates that this inhibitor blocks some proteolytic activity of short peptides, presumably products of upstream proteolytic activities. Here the authors argue, that because many of these detected short (di-/tri-) peptides could be mapped on the hemoglobin protein sequence, this must be their origin. Although this might be the case the author could not exclude the fact that at least some of these come from other sources (e.g. Plasmodium proteins). It would be quite helpful to comment on such a possibility as well. In particular, it was mentioned that the main subcellular localization of PfM1 is in the cytoplasm while most if not all hemoglobin digestion occurs in the digestive vacuole…?*

Indeed, we agree that _Pf_A-M1 is likely processing both Hb and non-Hb peptides and do not definitively conclude that all dysregulated peptides must be derived from haemoglobin. A subset of dysregulated peptides cannot be mapped to haemoglobin and must have an alternative source such as other host proteins or turnover of parasite proteins. We have amended the discussion to better reflect these possible alternate peptide sources (480-482). Although the peptides detected in the metabolomics study (2-5 amino acids) are too short to be definitively assigned to any specific parasite or RBC protein, it is important to note that our analysis strongly indicates that the majority, but not all, of dysregulated peptides are more likely to originate from haemoglobin than other human or parasite proteins. This is based on sequence mapping, which was aided by acquiring MS/MS data for a subset of dysregulated peptides from which we derive accurate sequences (as opposed to residue composition inferred from total peptide mass) to more directly link dysregulated peptides to haemoglobin. We further quantified the sequence similarity of dysregulated peptides to all detectable proteins in the *P. falciparum* infected erythrocyte proteome (~4700 proteins), showing that these peptides are statistically more similar to haemoglobin than other host or parasite proteins.

The apparent disconnect between PfA-M1 localisation (cytosol) and the predominant site of haemoglobin digestion (digestive vacuole, DV) is explained by the fact that peptides originating from digestion of haemoglobin in the DV are required to be transported into the

cytoplasm for further cleavage by peptidases, including PfA-M1. This point has now been clarified in the discussion (lines 473-474).

> ***Reviewer #3 (Recommendations For The Authors):***
>
> *(1) Thermal stability studies confirmed that PfA-M1 was a binding target, however, there were other proteins consistently identified in the thermal stability studies. This raises the question as to their potential role as additional targets of this inhibitor. The authors dismiss these because they are not metalloproteases, but further analysis is warranted. This is particularly important as the authors were not able to generate mutants using in vitro evolution of resistance strategies. This often indicates that the inhibitor has more than one target.*

We thank the reviewer for this comment. The possibility of other targets contributing to MIPS2673 activity was also raised by Reviewer #2 (question 2) and is addressed above. Further to our response to Reviewer #2, we agree that the inability to generate resistant parasites *in vitro* could indicate that inhibition of multiple essential parasite proteins (including PfA-M1) contribute to MIPS2673 activity and do not rule out this possibility. It may also indicate the target has a very high barrier for resistance and is unable to tolerate resistance causing mutations as they are deleterious to function. Indeed, previous attempts to mutate PfA-M1 (references 12 and 50), and our own attempts to generate MIPS2673 resistant parasites *in vitro* (unpublished), were unsuccessful. It is important to note that of the hits reproducibly identified using thermal stability proteomics, only PfA-M1 and a putative AP2 domain transcription factor (PF3D7_1239200) are predicted to be essential for blood stage growth. We have explicitly stated that PF3D7_1239200 could also contribute to activity (line 533 and 537).

As we identified multiple hits with thermal stability proteomics we employed the complementary LiP-MS method to further investigate the target landscape of MIPS2673. PfA-M1 was the only protein reproducibly identified as the target through this approach. Importantly, the five proteins identified as hits by thermal stability proteomics were also detected in our LiP-MS datasets, but only PfA-M1 was identified as a target by both target deconvolution methods, strongly indicating it is the primary target of MIPS2673 in parasites. An important caveat is that we profiled the soluble proteome (we did not include detergents necessary for extracting membrane proteins as they may interfere with these stability assays) and other factors (e.g. the biophysical properties of the protein) will impact on whether ligand induced stabilisation events are detected. We have added additional text in the discussion around the above points (lines 545-550).

While we do not definitively rule out other MIPS2673 interacting proteins existing in parasites (that possibly also contribute to activity), our metabolomics studies indicated no functional impact by MIPS2673 outside of elevated levels of short peptides. This is indicative of aminopeptidase inhibition and the profile of peptide accumulation was distinct from a known PfA-M17 inhibitor, and other antimalarials, further pointing to selective inhibition of the PfA-M1 enzyme by MIPS2673 being responsible for antimalarial activity.

> *(2) The next set of experiments focused on a limited proteolysis approach. Again several proteins were identified as interacting with MIPS2673 including metalloproteases. The authors go on to analyze the LiP-MS data to identify the peptide from PfA-M1 which putatively interacts with MIPS2673. The authors are clearly focused on PfA-M1 as the target, but a further analysis of the other proteins identified by this method would be warranted and would provide evidence to either support or refute the authors' conclusions.*

As PfA-M1 was the only protein reproducibly identified as an interacting protein across both LiP-MS experiments (and by thermal stability proteomics) we focused our analysis on this protein. However, we agree that further analysis of the other putative interacting proteins would be valuable. Additional analysis was performed (see new figure S4) on the other interacting proteins identified by thermal stability proteomics and the other interacting proteins identified in LiP-MS experiment one, as no other proteins (apart from PfA-M1) were identified as hits in the second LiP-MS experiment (lines 314-318, 495-505, 740-762 and Fig. S4). Using the common peptides detected across both LiP-MS experiments we mapped significant LiP peptides to the structures of the other putative MIPS2673-interacting proteins, where a structure was available and significant LiP-MS peptides were detected, and measured the minimum distance to expected binding sites. It is noted that when using the same criteria for a significant LiP peptide that we used for our PfA-M1 analysis, only one significant LiP peptide is identified from these other putative interacting proteins (YSPSFMSFK from PfADA). Therefore, we used a less stringent criteria for defining significant LiP peptides for these other proteins (see methods and Fig. S4 legend) in order to identify significant LiP peptides to map to structures. This analysis showed that, with the exception of PfA-M17, significant LiP-MS peptides for these other proteins are not significantly closer to binding sites than all other detected peptides, supporting our assertion that these other proteins are likely to be false positives or not functionally relevant MIPS2673 interacting proteins. Although significant peptides from PfA-M17 were closer to the binding site, our thermal stability and metabolomics data, combined with our previous work on the PfA-M17 enzyme, argue against this being a functionally relevant target (see lines 362-374 and 486-529 for a more detailed discussion). Another possible explanation for this result is that peptide substrates accumulating due to primary inhibition of PfA-M1 interact with PfA-M17, leading to structural changes around the enzyme active site that are detected by LiP-MS.

> *(3) The final set of experiments was an untargeted metabolomics analysis. They identified 97 peptides as significantly dysregulated after MIPS2673 treatment of infected cells and most of these peptides were derived from one of the hemoglobin chains. The accumulation of peptides was consistent with a block in hemoglobin digestion. This experiment does reveal a potential functional confirmation, but questions remain as to specificity.*

As indicated, the accumulation of short peptides identified by metabolomics suggests MIPS2673 perturbs aminopeptidase function. Many of these peptides (but not all) likely map to haemoglobin and are more haemoglobin-like than other proteins in the infected red blood cell proteome. An effect on a subset of non-haemoglobin peptides is also apparent and we have added this to our discussion (also refer to our response to question 4 from Reviewer #2). A direct comparison to our previous metabolomics analysis of a specific PfA-M17 inhibitor (MIPS2571, reference 11) revealed MIPS2673 induces a unique metabolomic profile. The extent of peptide accumulation differed and a subset of short basic peptides (containing Lys or Arg) were elevated only by MIPS2673, consistent with the broad substrate preference of PfA-M1. Importantly, the metabolomics profile induced by MIPS2673 is the opposite of many other antimalarials, which cause depletion of haemoglobin peptides. Taken together, the profile of short peptide accumulation induced by MIPS2673 is consistent with specific inhibition of PfA-M1.

> *(4) Overall, this is an interesting series of experiments that have identified a putative inhibitor of PfA-M1 and PvA-M1. The work would be significantly strengthened by structure-aided analysis. It is unclear why putative binding sites cannot be analyzed via specific mutagenesis of the recombinant enzyme.*

Contrary to this comment we solved the crystal structure of PfA-M1 bound to MIPS2673, determining its binding mechanism to the enzyme. This was further supported through proteomics-based structural analysis by LiP-MS. Undertaking site specific mutagenesis would be interesting to further probe the binding dynamics of MIPS2673 to the M1 protein. However, we believe it is beyond the scope of this study and would not change our conclusion that MIPS2673 binds to PfA-M1, which we have shown using multiple unbiased proteomics-based methods, enzyme assays and X-ray crystallography.

> *(5) In the thermal stability and LiP -MS analysis, other proteins were consistently identified in addition to PfA-M1 and yet no additional analysis was undertaken to explore these as potential targets.*

As addressed in our previous responses, across independent thermal stability proteomics experiments we consistently identified 5 interacting proteins, including the expected target PfA-M1. In contrast, only PfA-M1 was reproducible across independent LiP-MS experiments. While several plausible putative targets (including aminopeptidases and metalloproteins) were identified in one of our LiP-MS experiment, they appear to be false discoveries and not responsible for the antiparasitic activity of MIPS2673, as peptide-level stabilisation was not consistent across independent LiP-MS experiments, and an interaction is refuted by our thermal stability, metabolomics and recombinant enzyme inhibition data. We have now performed further analysis of these other putative interacting proteins, which also argues against them being likely interacting proteins (see also response to question 2). We have also added to our existing discussion on possible MIPS2673 targets and the likelihood of these proteins contributing to antimalarial activity (lines 486-550).

> *(6) The metabolomics experiments were potentially interesting, but without significant additional work including different lengths of treatment and different stages of the parasite, the conclusions drawn are overstated. Many treatments disrupt hemoglobin digestion - either directly or indirectly and from the data presented here it is premature to conclude that treatment with MIPS2673 directly inhibits hemoglobin digestion.*

Our metabolomics studies were performed using typical experimental conditions for investigating the antimalarial mechanisms of compounds by metabolomics (see references 11, 39, 40 and 55-57). We used a short 1 h incubation at 3x EC50 allowing us to profile the primary parasite pathways affected by MIPS2673 and avoid a nonspecific death phenotype associated with longer incubations. As addressed in our response to Reviewer #1 (question 2) we focused on trophozoite infected red blood cells as this is the stage most susceptible to MIPS2673 and when one presumes the greatest functional impact would be seen. It is possible that an expanded kinetic metabolomics analysis may reveal secondary mechanisms involved in MIPS2673 activity and we have now acknowledged this in the manuscript (lines 515-516). However, even though secondary mechanisms may become apparent at longer incubations it also becomes difficult to uncouple drug specific responses from nonspecific death effects. We believe any additional information provided by an expanded metabolomics analysis is unlikely to outweigh the significant extra financial cost associated with this type of experiment.

It is correct that many antimalarial compounds appear to disrupt haemoglobin digestion when analysed by metabolomics. However, as indicated in our manuscript (lines 369-373) and previous responses, the profile of elevated haemoglobin peptides induced by MIPS2673 is substantially different to the profile caused by other antimalarials. For example, artemisinins and mefloquine cause haemoglobin peptide depletion (references 55-57) and chloroquine results in increased levels of a different subset of non-haemoglobin peptides (see Creek et al. 2016). While there is some overlap in profile with a selective M17 inhibitor (our previous work, reference 11), the level of enrichment of these peptides is different and MIPS2673 also

induces accumulation of a distinct set of basic peptides consistent with the substrate preference of the PfA-M1 enzyme. As we show that MIPS2673 does not inhibit other parasite aminopeptidases, a likely explanation for the profile overlap is that the build-up of substrates that cannot be processed by PfA-M1 leads to secondary dysregulation of other aminopeptidases. Our analyses (sequence mapping, MS/MS analysis and sequence similarities to all infected red blood cell proteins) strongly indicate that the majority of elevated peptides (but not all) originate from haemoglobin. Combined with our proteomics and recombinant enzyme data indicating direct engagement of PfA-M1, and with previous literature indicating the enzyme functions to cleave amino acids from haemoglobin-derived peptides, our data indicates MIPS2673 likely directly perturbs the haemoglobin digestion pathway through PfA-M1 inhibition.

> *(7) Finally, the potency of this compound on parasites grown in vitro is 300 nM - this would need improvements in potency and demonstration of in vivo efficacy in the SCID mouse model to consider this a candidate for a drug.*

We do not propose MIPS2673 as an antimalarial candidate. The experiments presented here were centred on target validation rather than identification of an antimalarial lead, which may be the focus of future studies. To avoid this confusion, we have amended the manuscript title and language throughout to clarify this point.

https://doi.org/10.7554/eLife.92990.2.sa4